Acoustic Tracking and Characterization of Tornadoes

May 30, 2012

Joseph Park, PhD, PE, NOS/CO-OPS

OneNOAA Seminar
Sponsor: NOAA NOS Science Seminar Series and the NOS Center for Operational Oceanographic Products and Services (CO-OPS)

Remote Infrasonic Monitoring of Natural Hazards, NOAA National Weather Service Program Office (NWSPO) agreement number: NA08NWS4680044.

Selective History

1884: John Park Finley of the United States Army Signal Corps Issues Experimental Tornado Warnings.

1885: "It is believed that the harm done by such a prediction would eventually be greater than that which results from the tornado itself." (Report of the Chief Signal Officer 1887)

1905 – 1934: Weather Bureau Station Regulations contained the statement: "Forecasts of tornadoes are prohibited."

Bradford, M., 1999: Historical Roots of Modern Tornado Forecasts and Warnings. *Wea. Forecasting*, **14**, 484–491.

Coleman, T. A., Pence, K. J., 2009: The Proposed 1883 Holden Tornado Warning System. *Bull. Amer. Meteor. Soc.*, **90**, 1789–1796

Selective Statistics

1986 to 1995 : 49% of tornado fatalities were unwarned.
1996 to 2007 : 11.4% of tornado fatalities were unwarned.

2000 to 2004 : 26% of all reported tornadoes across the United States occurred without a NWS warning.
For Singular Events - over 50% were not warned.

During 2008 approximately 75% of tornado warnings issued by the National Weather Service (NWS) were unable to be confirmed as having produced a tornado.

Black, A. W., Walker, S. A., 2011: The Relationship between Tornadic and Nontornadic Convective Wind Fatalities and Warnings. *Wea. Climate Soc.*, **3**, 31–47.

Brotzge, J., Erickson, S., Brooks, H., 2011: A 5-yr Climatology of Tornado False Alarms. *Wea. Forecasting*, **26**, 534–544.

National Weather Service, 2009: Storm-based warnings: A presentation for NOAA's NWS managers.

Acoustics

20Hz

Infrasound

20Hz

Audible

Human Voice

20 kHz

Ultrasound

20 kHz

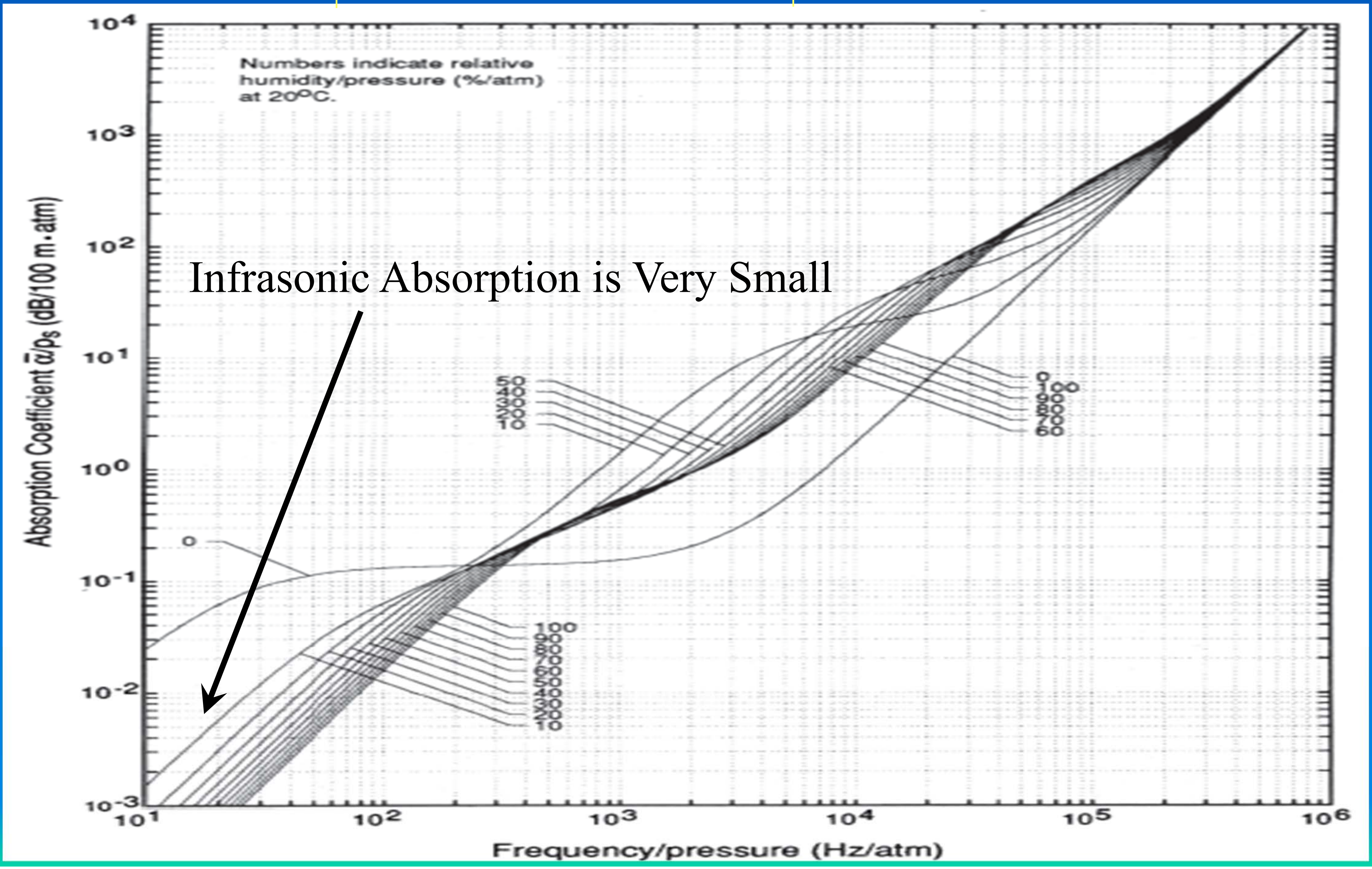

Infrasonic wavelengths in air range from meters to kilometers

Frequency (Hz)	Wavelength (m)
0.01	34,300
0.1	3,430
1	343
10	34.3
100	3.43
1000	0.34
10000	0.034

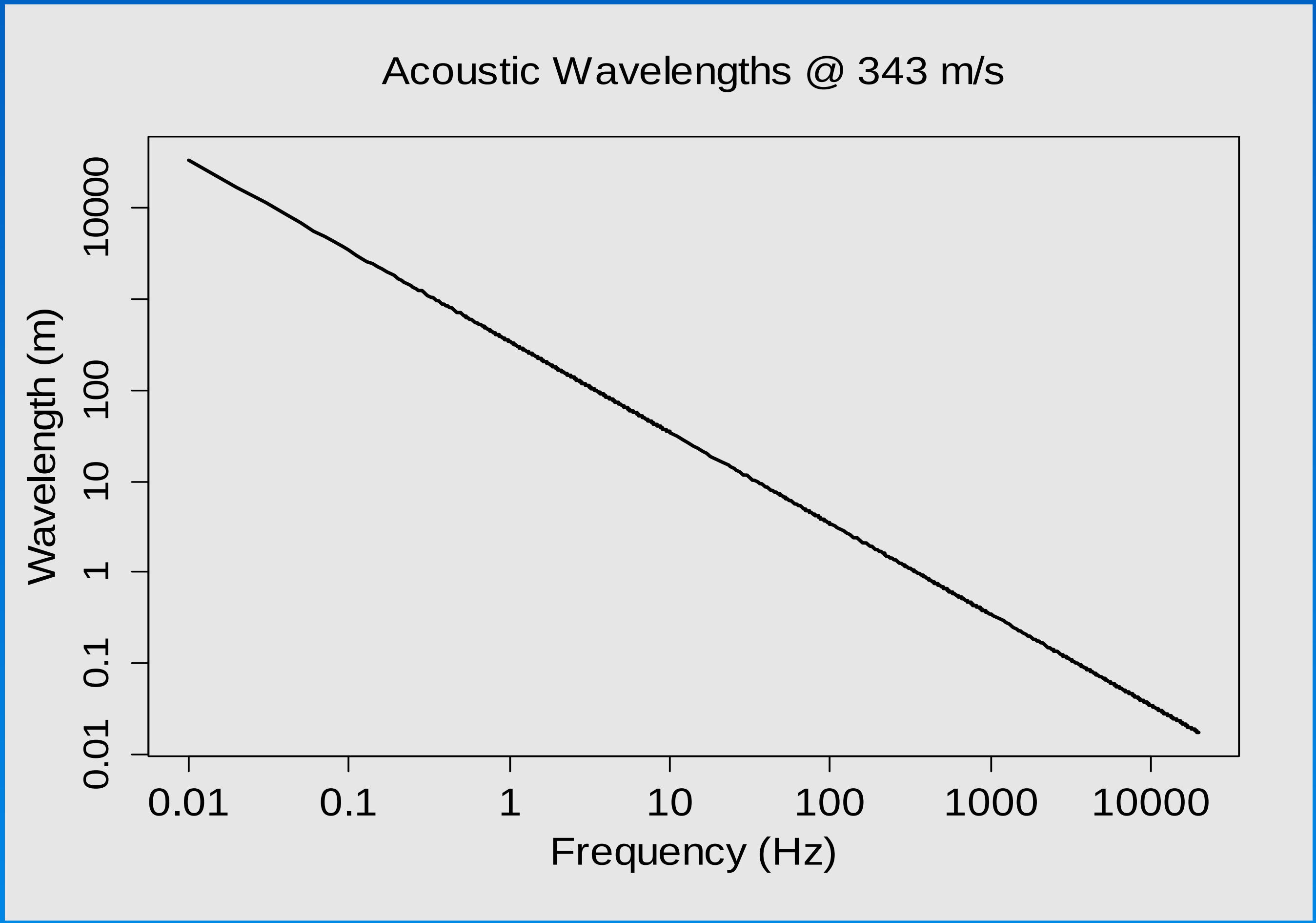

Meteorological conditions govern the Effective Sound Speed, which determines the propagation characteristics of acoustic energy.

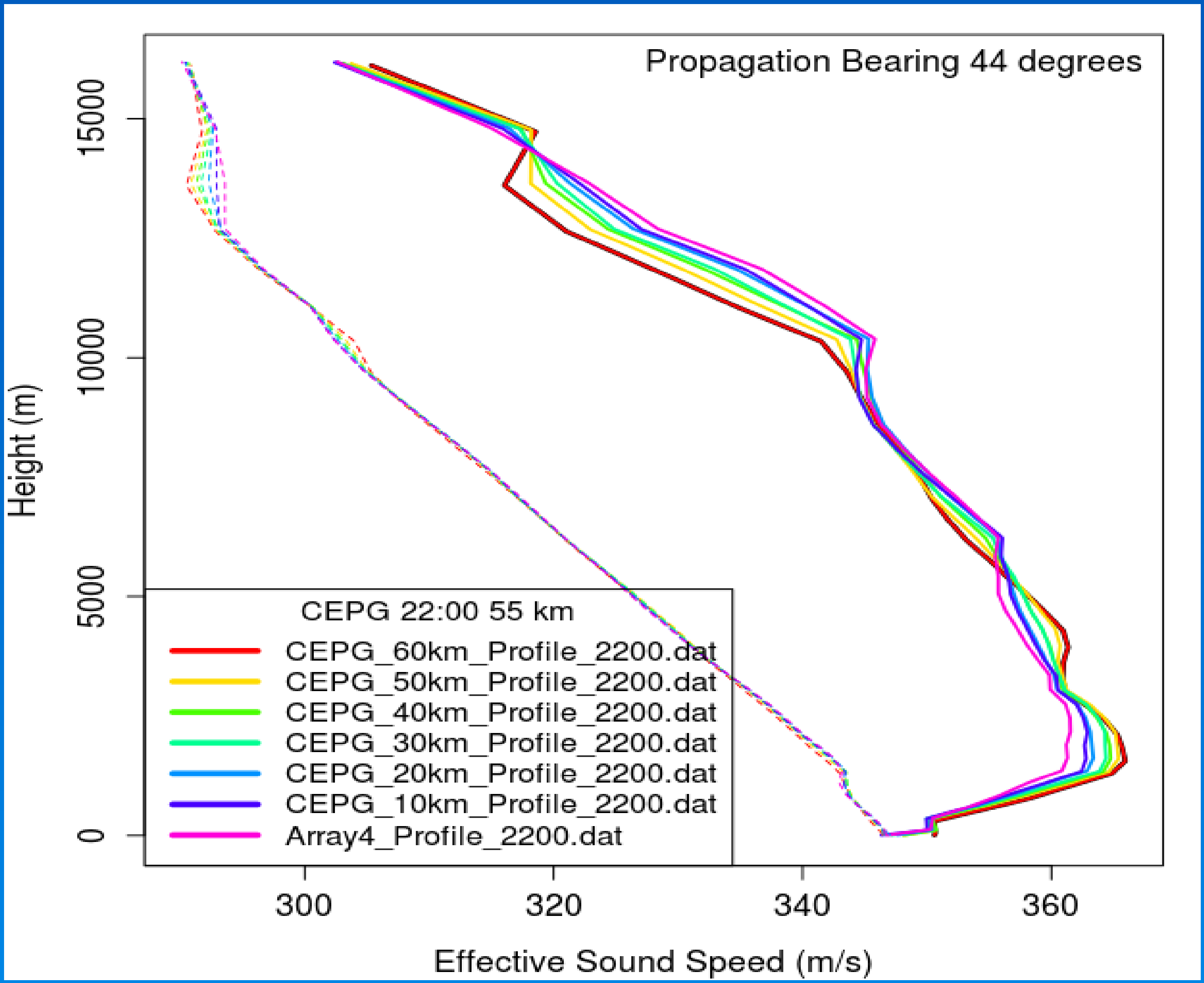

Sound Speed:
340 m/s : 760 mph

Storm Speeds
10 m/s : 22 mph
15 m/s : 33 mph
25 m/s : 56 mph

Parabolic Wave Equation solution for CEPG Tornado conditions.

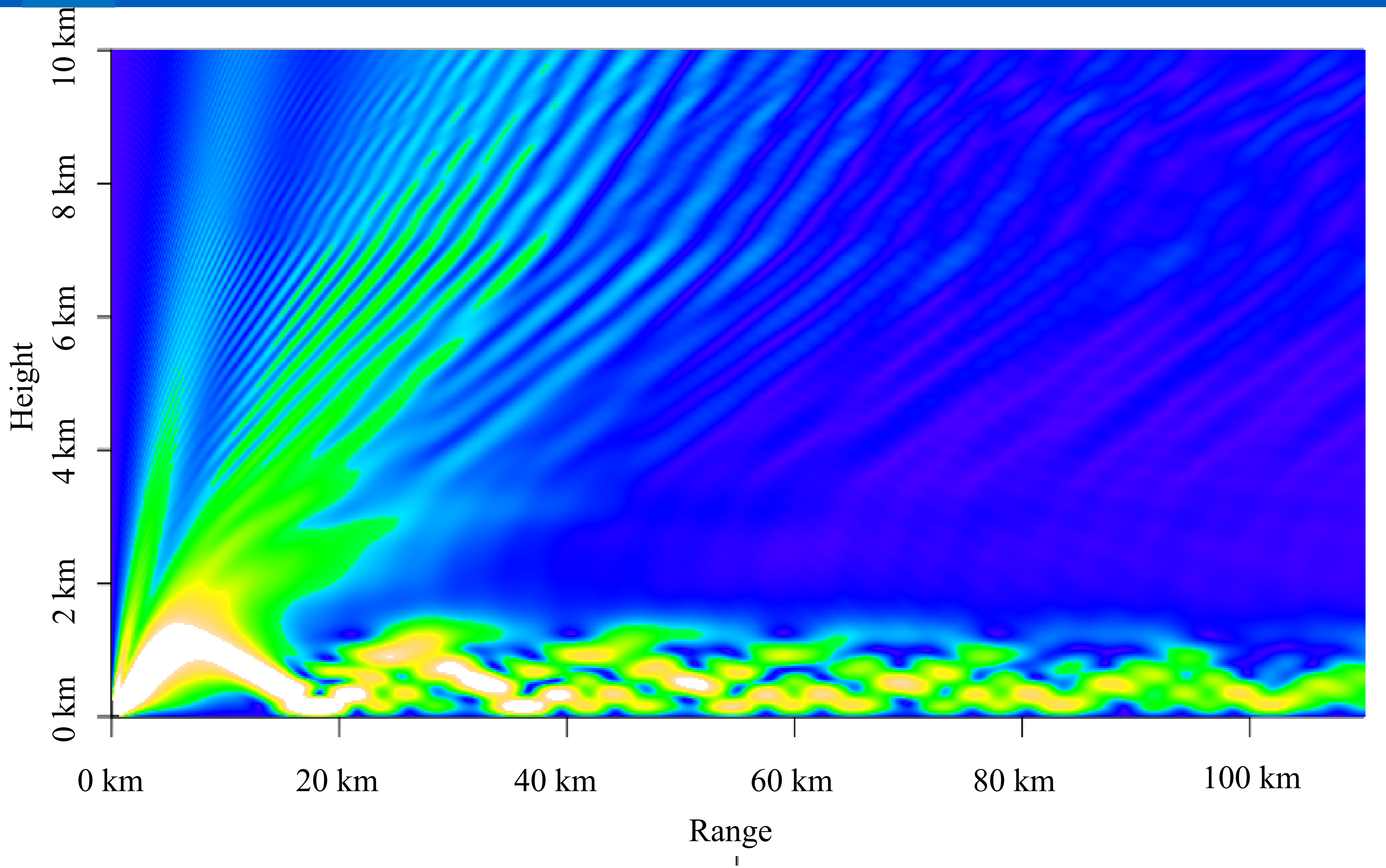

The first record of naturally occurring infrasound was the 1883 eruption of the Krakatoa volcano in Indonesia. Infrasonic waves circled the Earth 7 times.

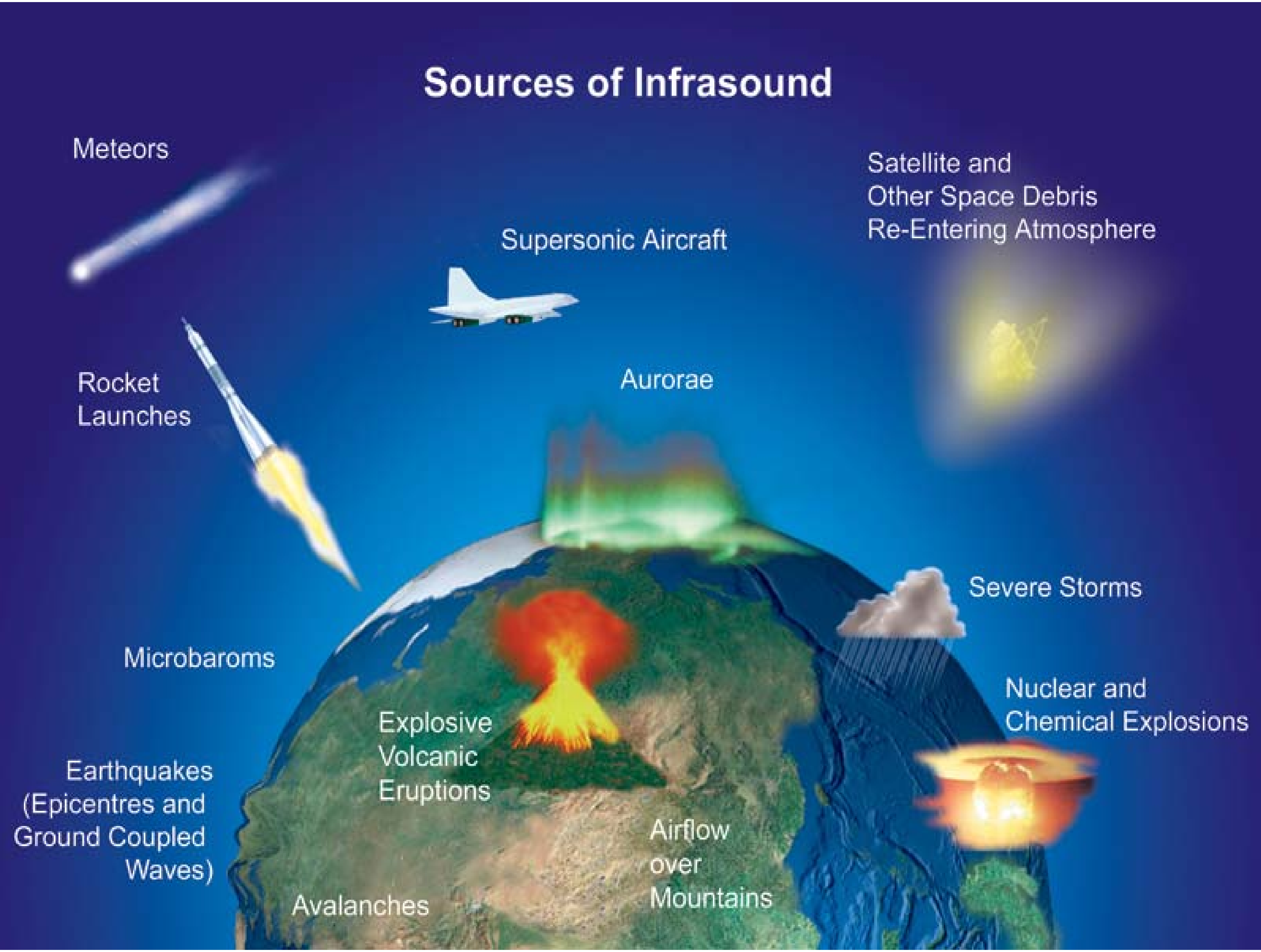
Sources of Infrasound
Meteors
Satellite and Other Space Debris Re-Entering Atmosphere
Supersonic Aircraft
Rocket Launches
Aurorae
Severe Storms
Microbaroms
Nuclear and Chemical Explosions
Explosive Volcanic Eruptions
Earthquakes (Epicentres and Ground Coupled Waves)
Airflow over Mountains
Avalanches

Comprehensive Nuclear-Test-Ban Treaty (CTBT)

Bans nuclear explosions by everyone, everywhere: on the Earth's surface, in the atmosphere, underwater and underground.

CTBT IMS Research & Development led to significant improvements in infrasound sensing technology.

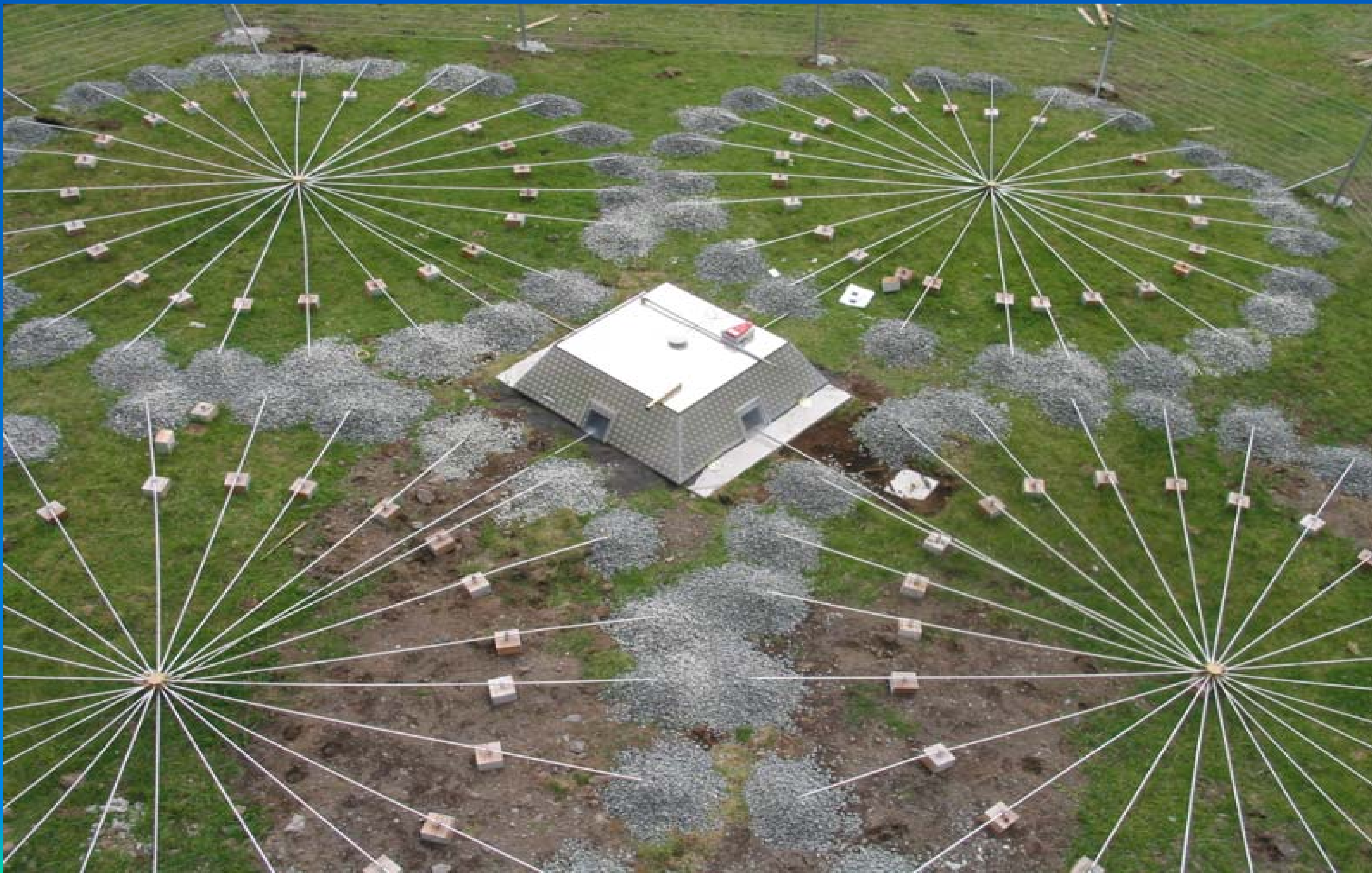

Al Bedard & T. M. Georges Pioneered the use of CTBT Infrasound technology to detect and monitor severe weather: http://www.esrl.noaa.gov/psd/programs/infrasound/isnet/

InfraSonics Network: IS Net

The Infrasonics Network is a prototype system to assess the possibility of improving warnings of severe weather events. Based upon a decade of study at ETL, IS Net was deployed in the summer of 2003 to evaluate it's capability to provide advance warning of tornadoes.

VORTEX SOUND GENERATION

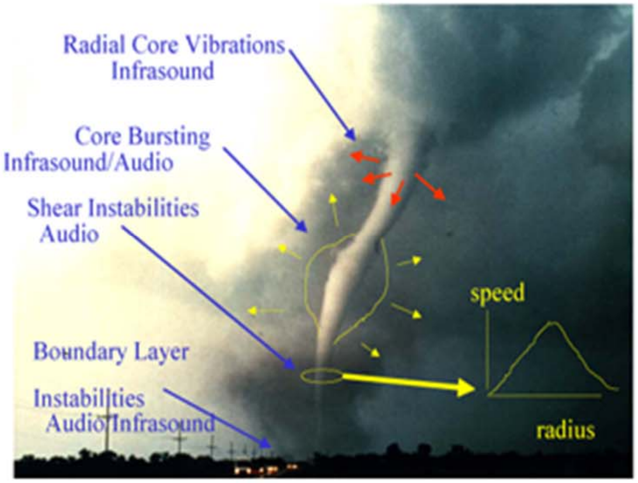

How can infrasonic observatories improve tornado warnings?

- Provide vortex detection capabilities where radar constraints exist (e.g. obstacle blocking, longer ranges where radar resolution is degraded, short ranges where high elevation radar scans are limited).
- Provide detection continuity between radar scans (The interval between consecutive Nexrad volume scans is 5 minutes).
- Provide information on smaller diameter vortices.
- Provide information on vortices of limited vertical extent, which may not show clearly on volume scan displays.
- Potentially provide guidance for optimizing radar scans.
- Provide information on vortex core size (using the sound generation model of Abdullah, 1966).

IS Net Demonstration Array

Contact: alfred.j.bedard@noaa.gov

1. Provide vortex detection capabilities where radar constraints exist.
2. Provide detection continuity between radar scans.
3. Provide information on smaller diameter vortices.
4. Provide information on vortices of limited vertical extent, which may not show clearly on volume scan displays.
5. Potentially provide guidance for optimizing radar scans.
6. Provide information on vortex core size (using the sound generation model of Abdullah, 1966).

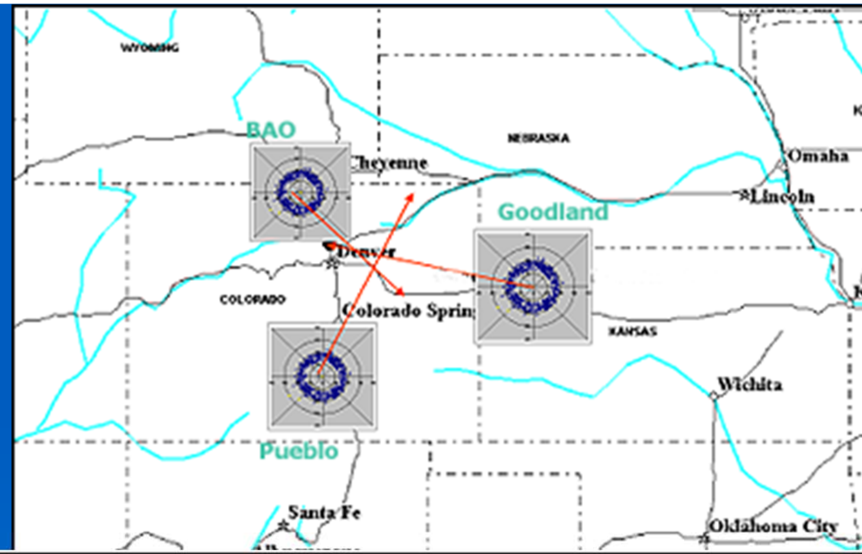

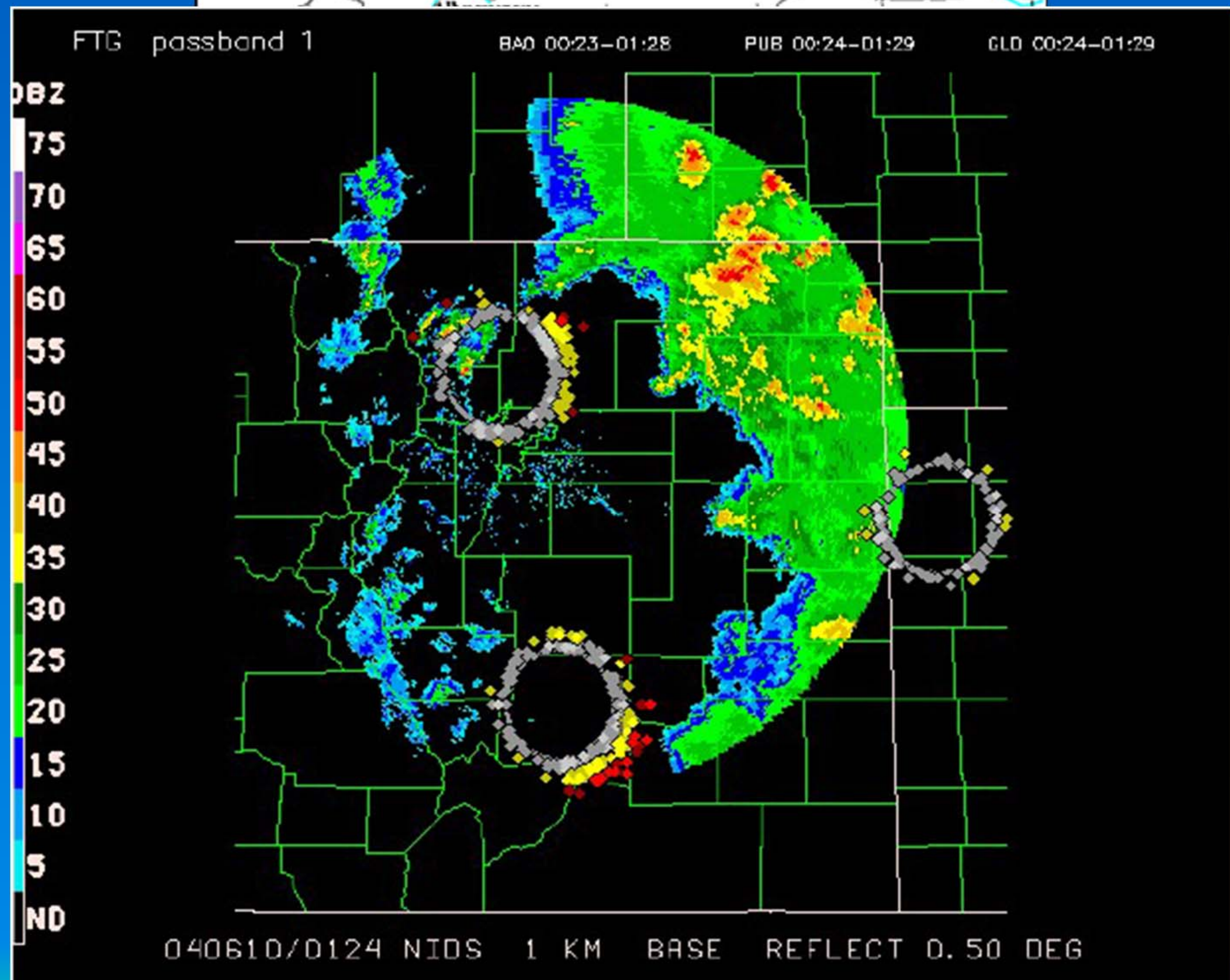

FIG. 21. Standard web display on 10 June 2004 near the time of a tornado report in NE Colorado.

NCPA Developed a Revolutionary Infrasound Sensor

Wide Dynamic Range & Frequency Response
Ruggedized
Self Contained, Low Power
Internal ADC, Linux Kernel, uProcessor, Data Storage, 802.11 WiFi

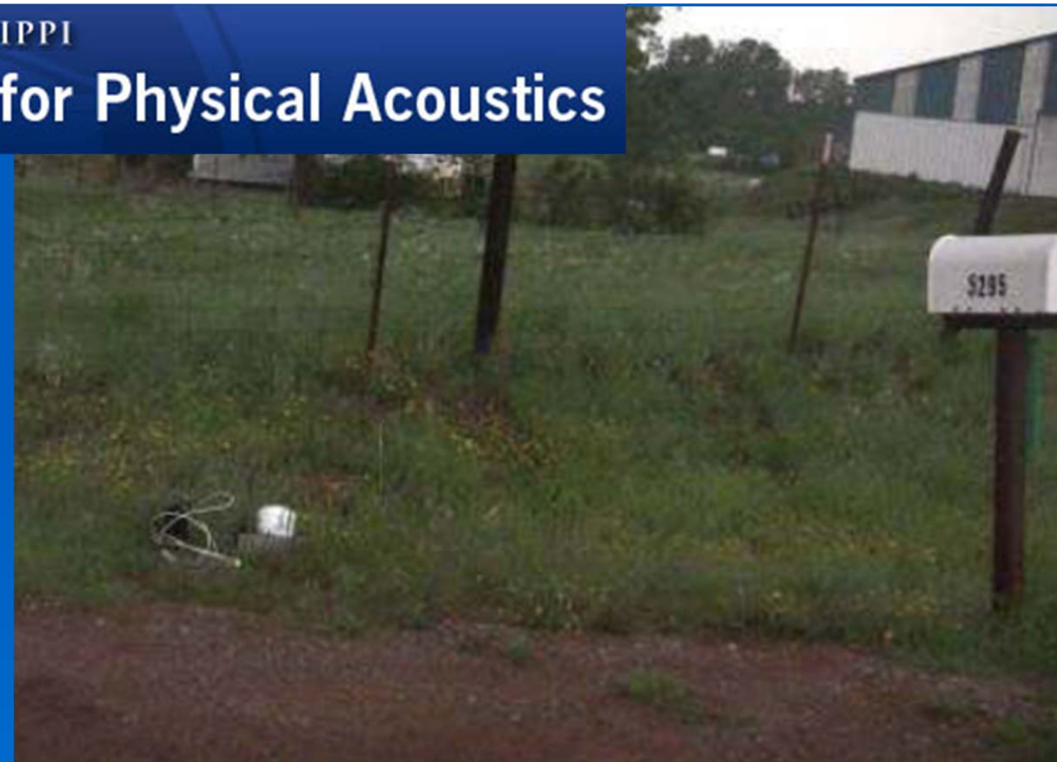

Contact Dr. Roger Waxler: rwax@olemiss.edu

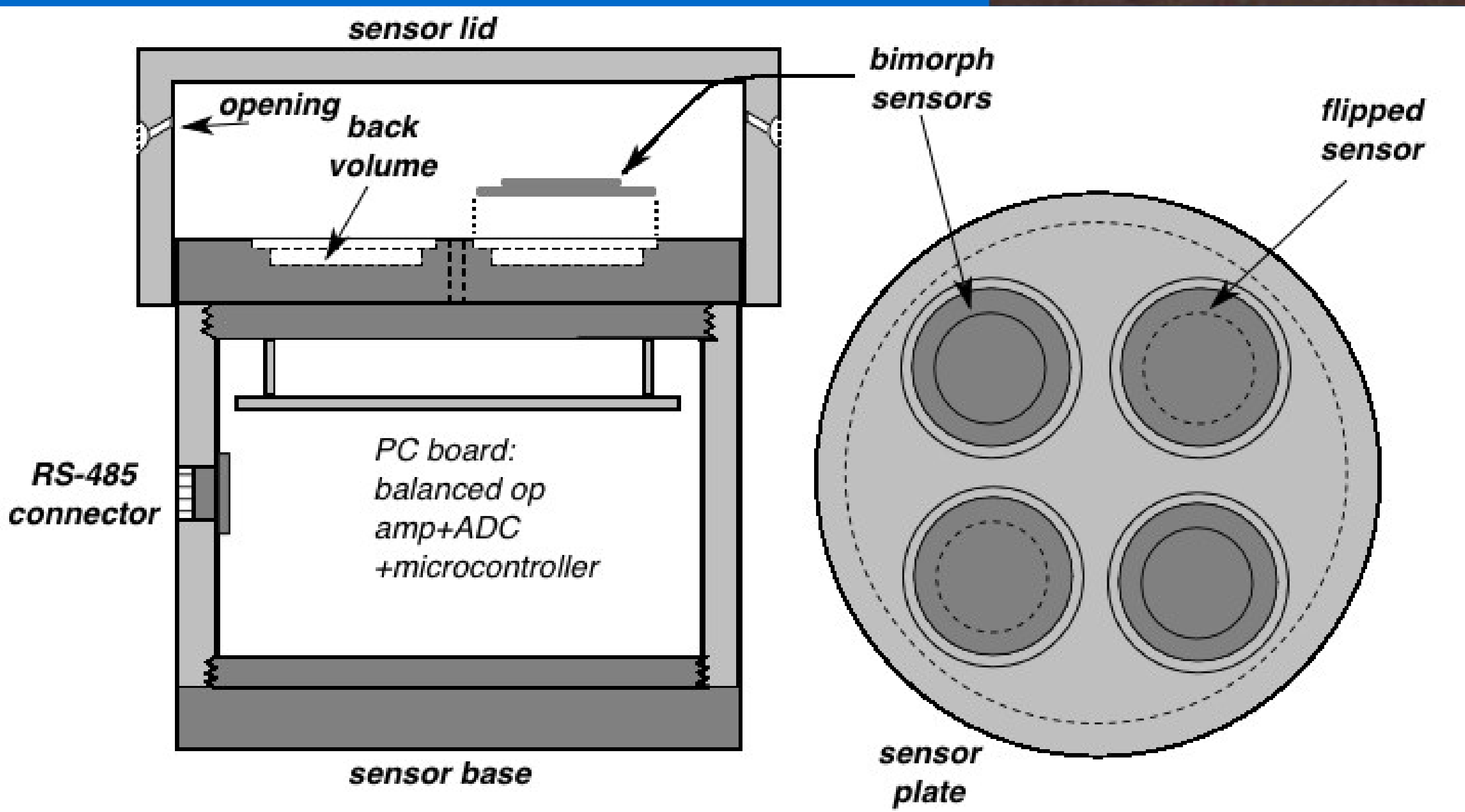

Tornado tracks from the May 24, 2011 Tornado Outbreak in Oklahoma. The approximate location of infrasound sensor arrays is shown by the red circles, three storms analyzed from this outbreak are labeled.

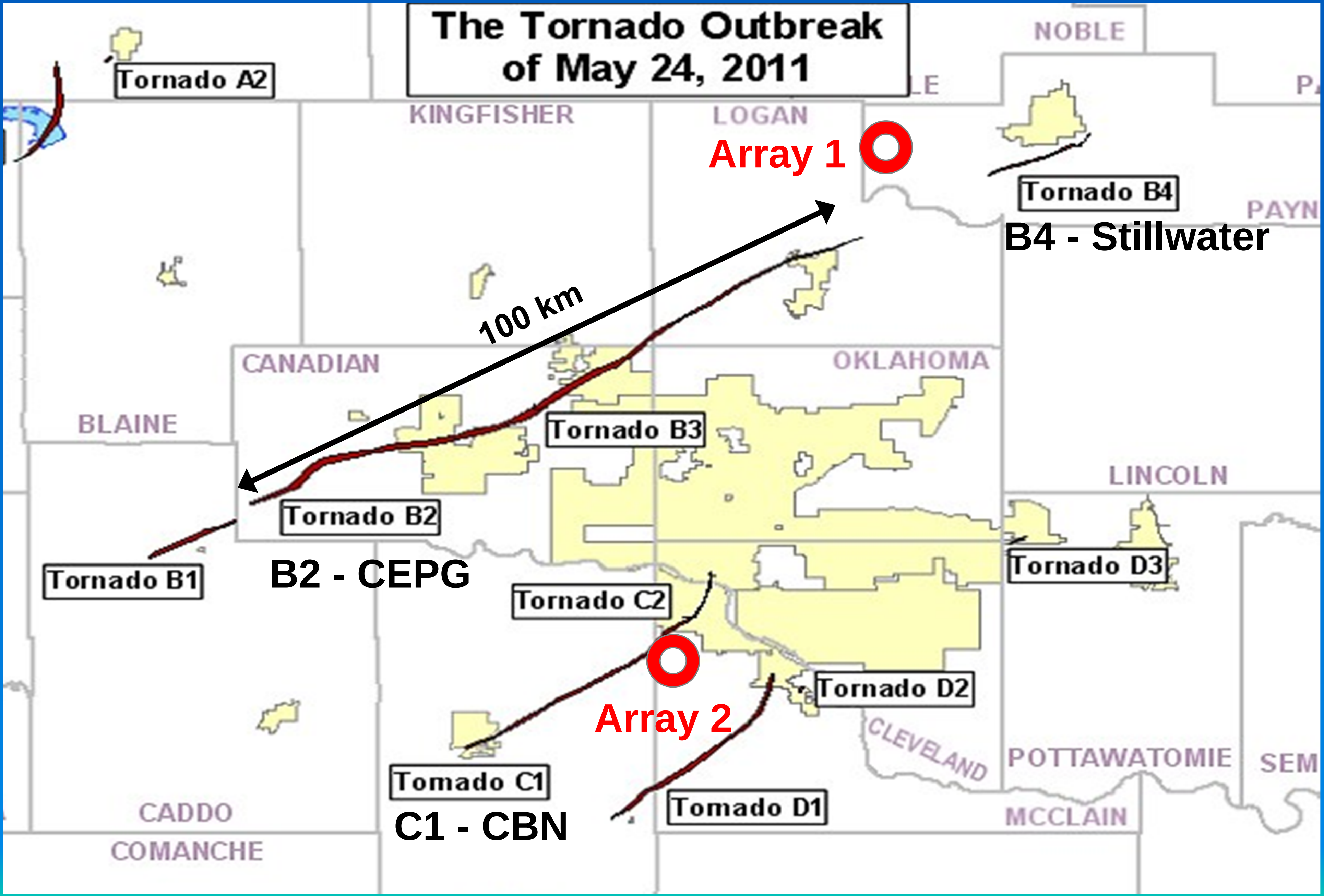

The Calumet-El Reno-Peidmont-Guthrie (CEPG) tornado of May 24, 2011, Oklahoma.

Duration:	1 hour 45 minutes
Path Length:	100 kilometers, width 1.6 km
Estimated Winds:	94 m/s (210 mph)
Damage Rating:	EF-5, 9 fatalities, 181 injuries

Damage from the Calumet-El Reno-Peidmont-Guthrie (CEPG) tornado of May 24, 2011.

The Chickasaw-Blanchard-Newcastle (CBN) tornado of May 24, 2011, Oklahoma.

Duration:	55 minutes
Path Length:	51.5 km, width 800 m
Estimated Winds:	85 m/s (190 mph)
Damage Rating:	EF-4, 1 fatality, 48 injuries

Damage from the Chickasaw-Blanchard-Newcastle (CBN) tornado of May 24, 2011, Oklahoma.

(a) Pressure measured from the CEPG analysis (22:15 - 22:30 UTC) on sensor SN089 of Array 1. Range to storm ~42 to 28 km.

(b) Finer time resolution of the large amplitude event in (a) marked with vertical lines. Times are UTC on May 24, 2011.

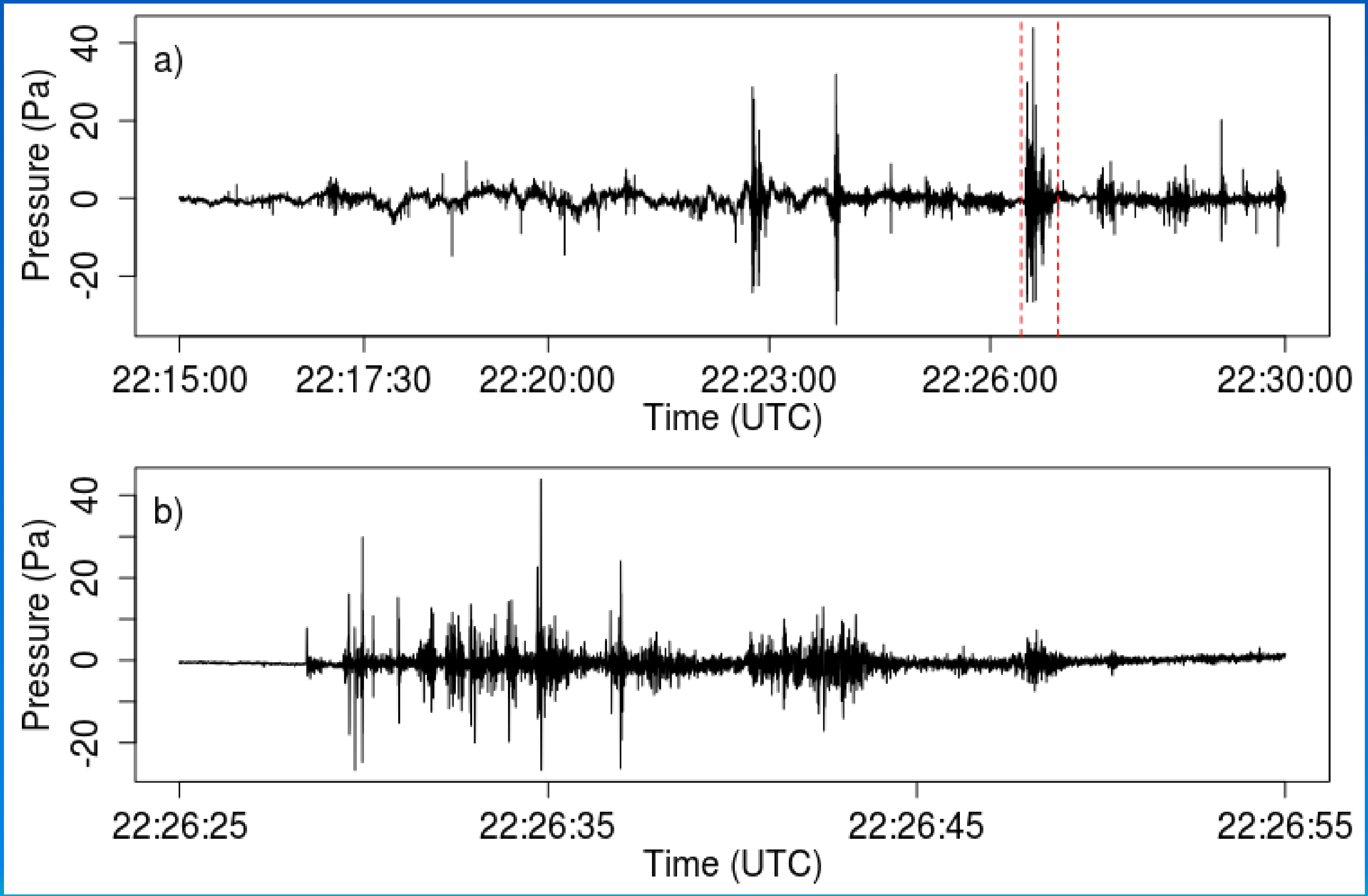

Power spectral density comparison of two tornadoes and a 'quiet time' when no tornadoes were present. Times are UTC on May 24, 2011.

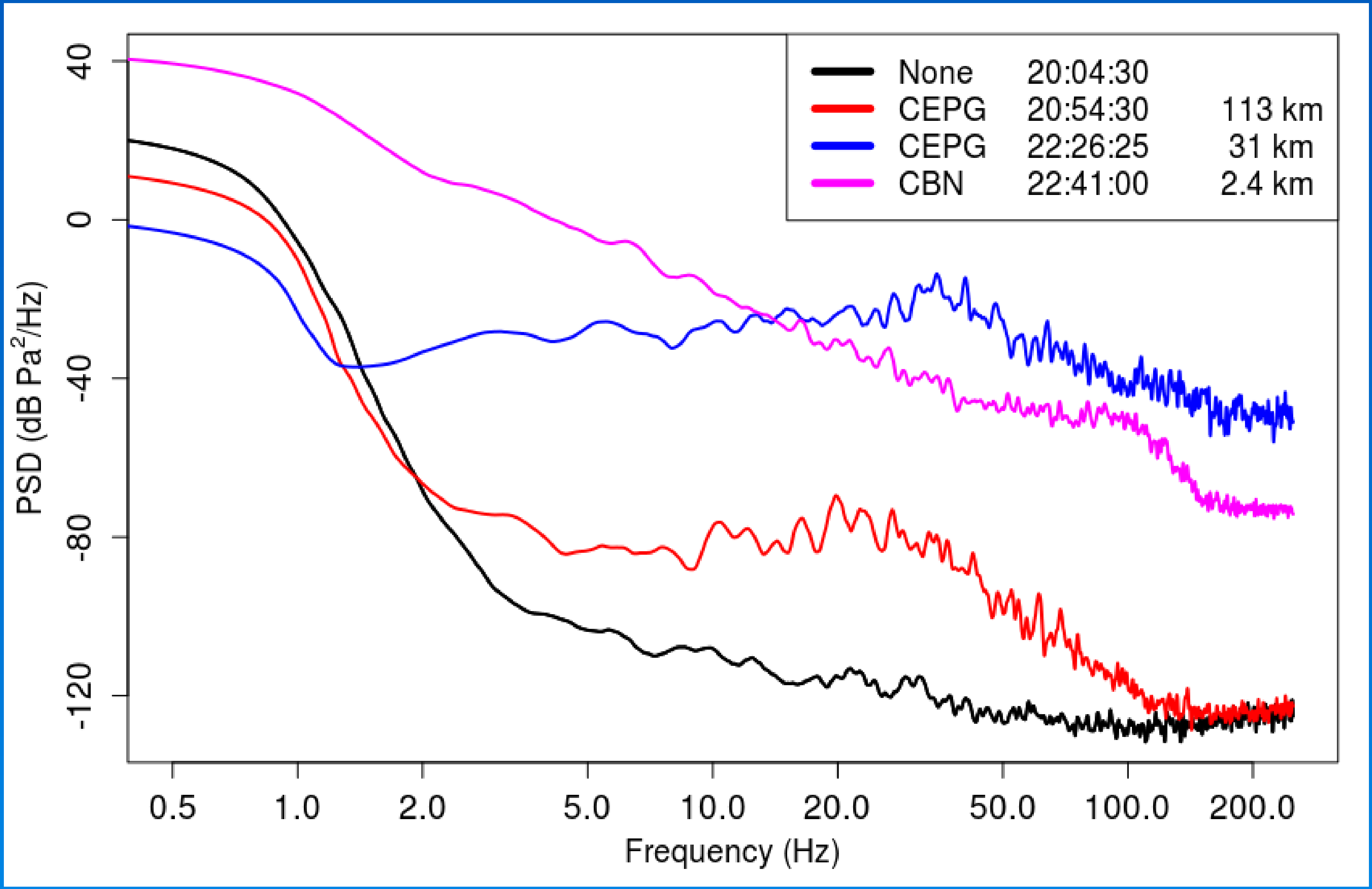

Pressure Ratios: 20 dB = 10, 40 dB = 100, 60 dB = 1000, 80 dB = 10000

Power spectral density averaged across 4 sensors of Array 1 for 30 second periods during the CEPG tornado. Times are UTC on May 24, 2011.

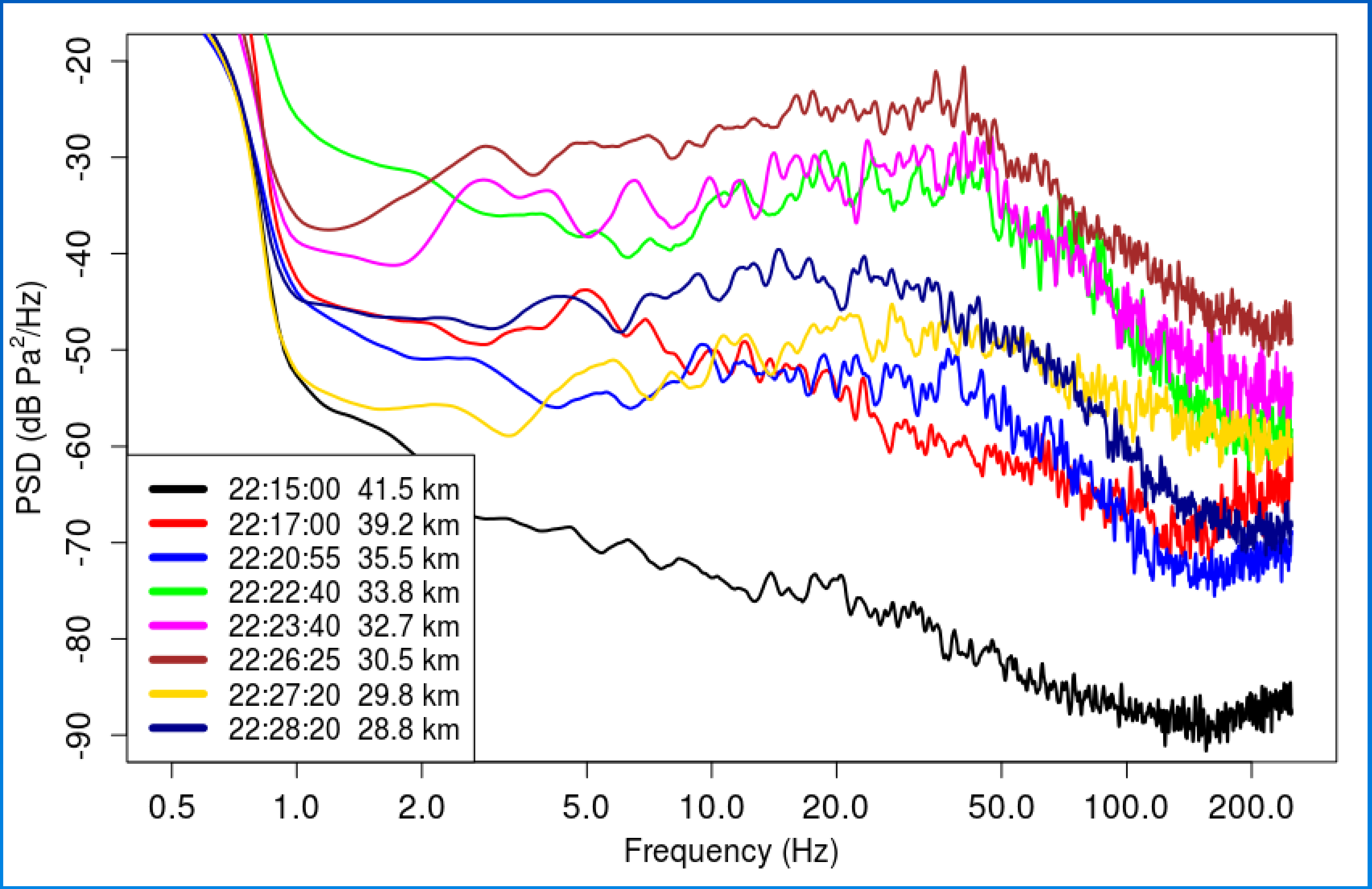

Single sensor power spectral density over 30 second periods during and after the CBN tornado. Times are UTC on May 24, 2011.

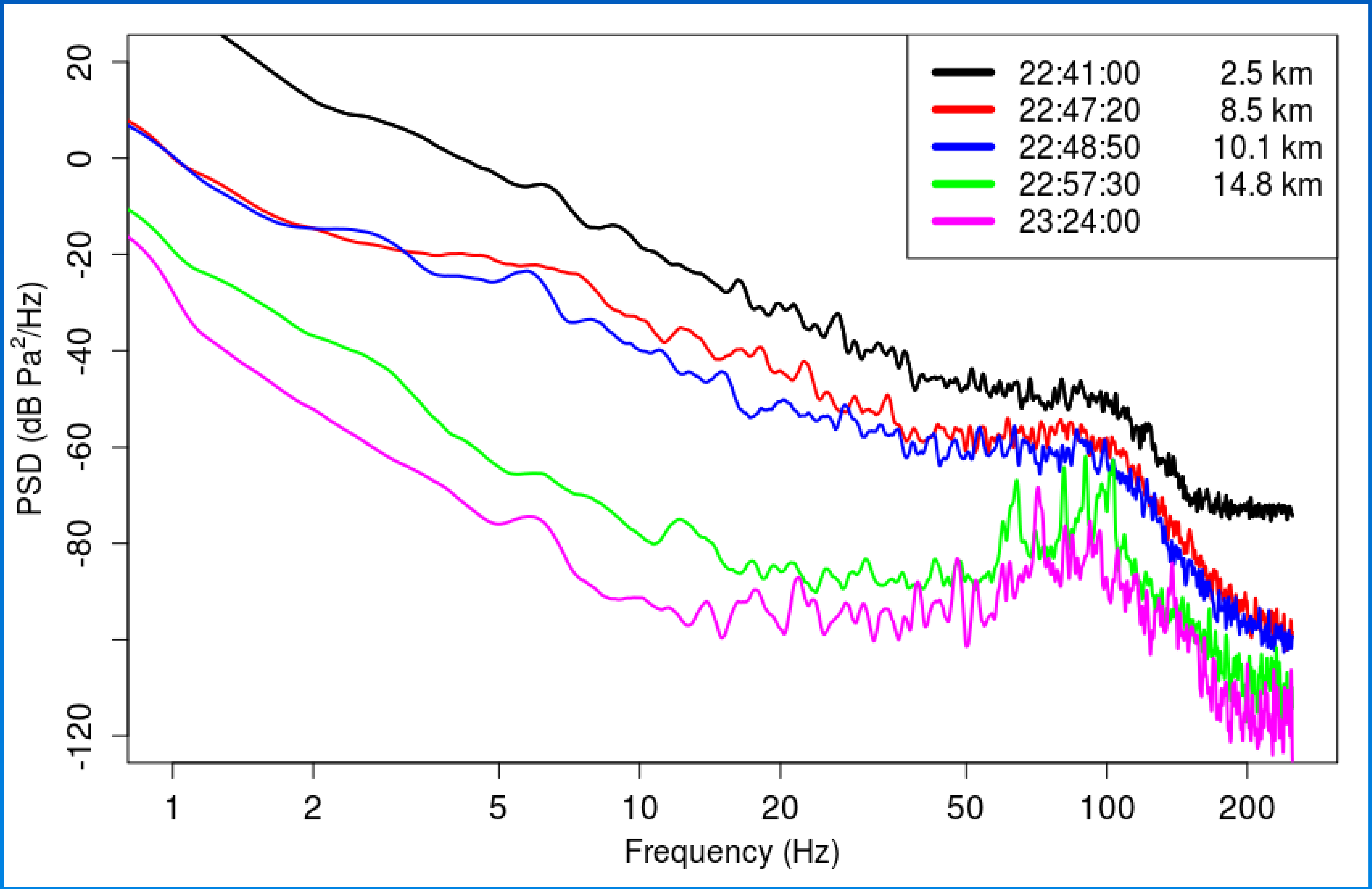

Single sensor power spectral density over 30 second periods between the CEPG and Stillwater tornadoes. Times are UTC on May 24, 2011.

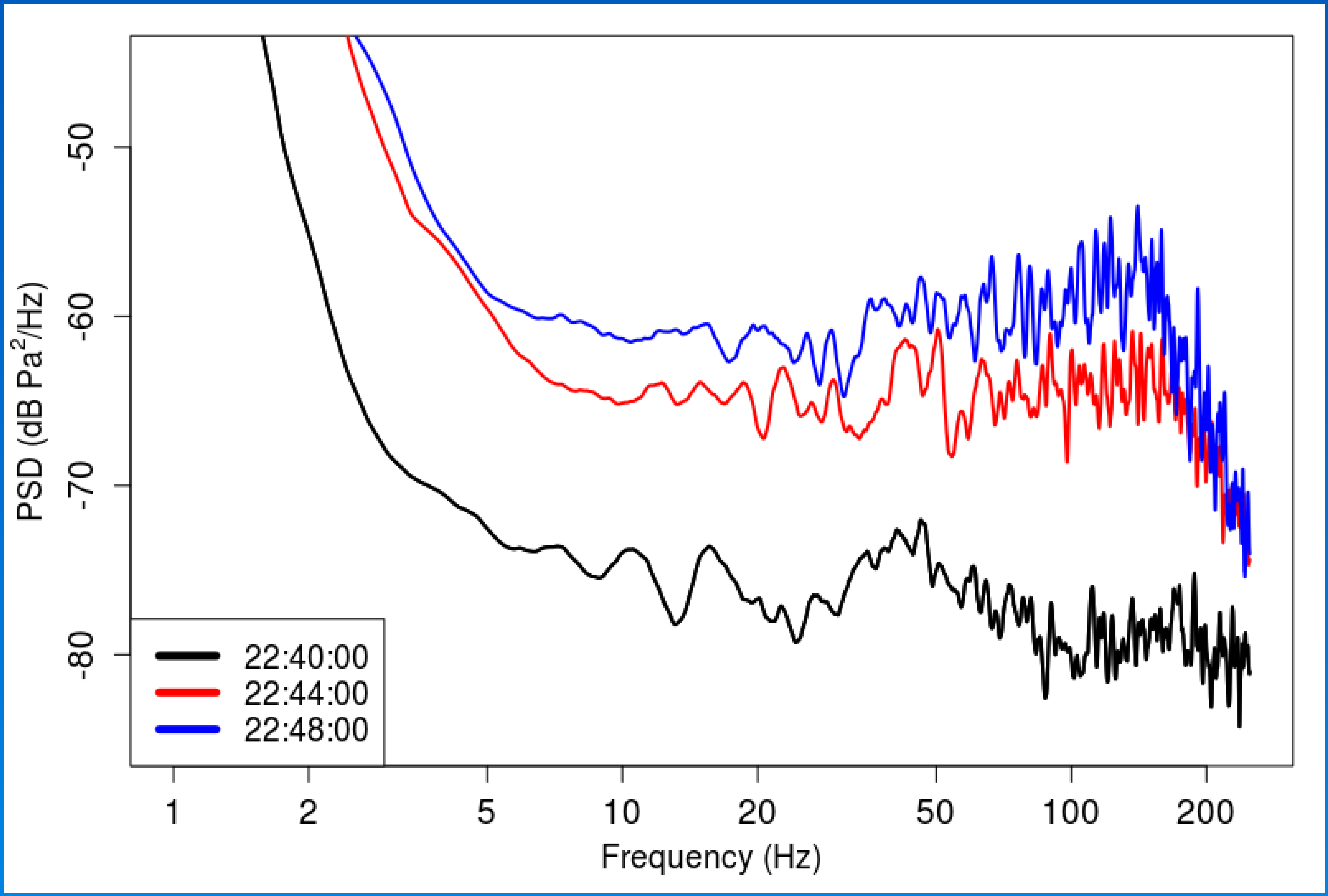

Effective sound speed computed from meteorological data at 2100 UTC on May 24th, approximately 50 km SSW of Array 1.

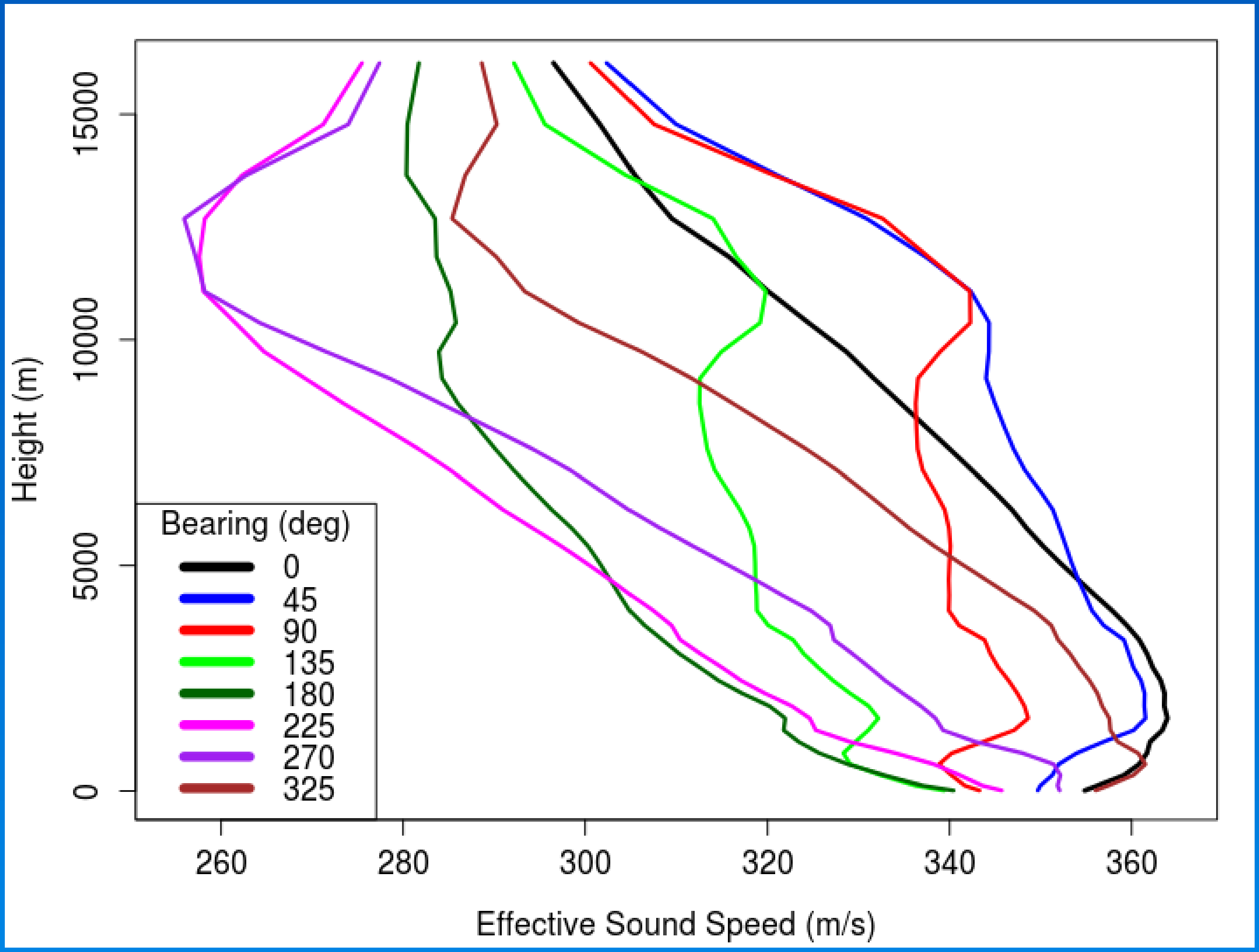

Acoustic transmission loss (TL) in dB at a frequency of 3 Hz from atmospheric data at 2100 UTC, May 24, 2011 approximately 50 km SW of Array 1.

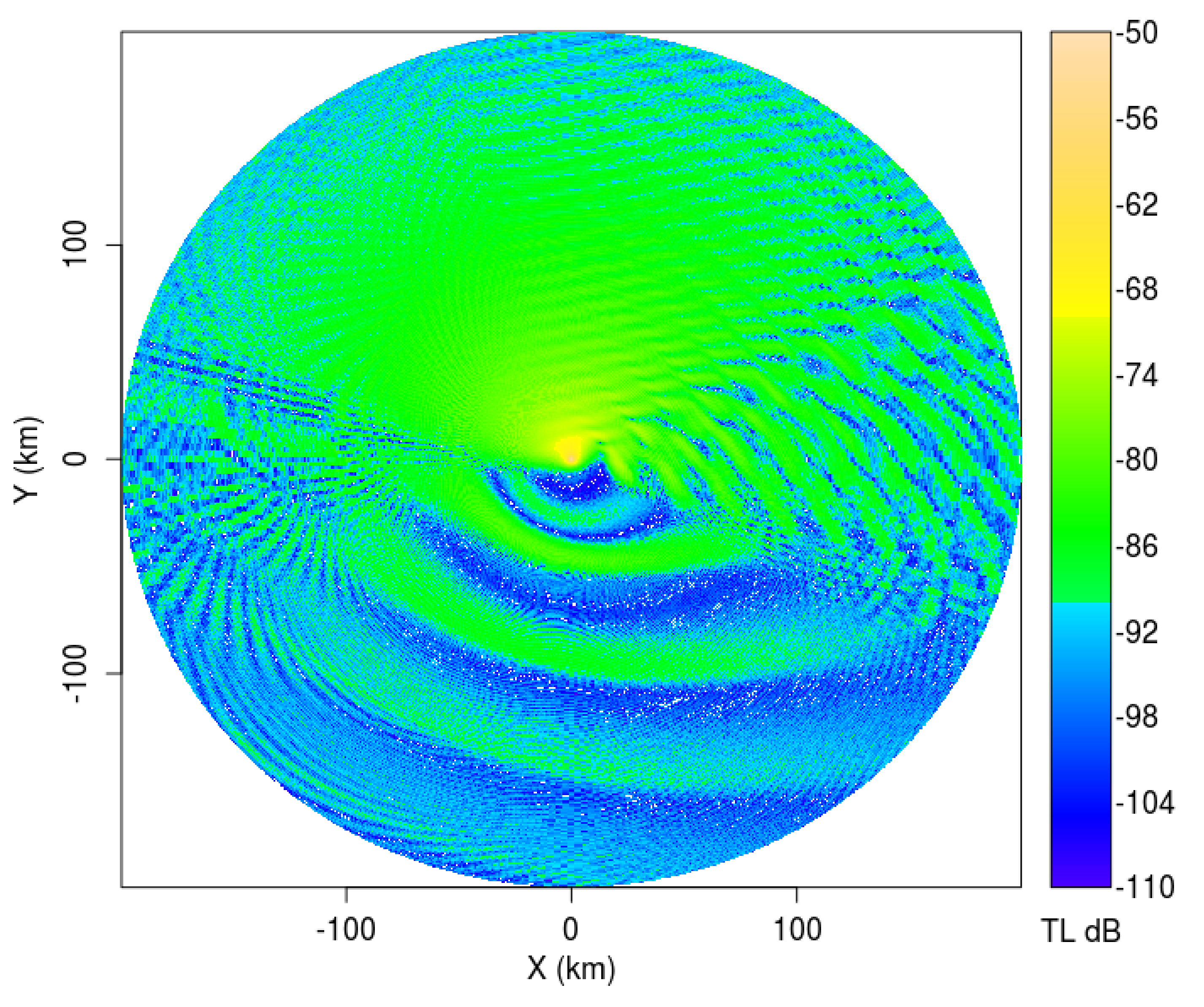

Acoustic transmission loss (TL) in dB at a frequency of 40 Hz from atmospheric data at 2100 UTC, May 24, 2011 approximately 50 km SW of Array 1.

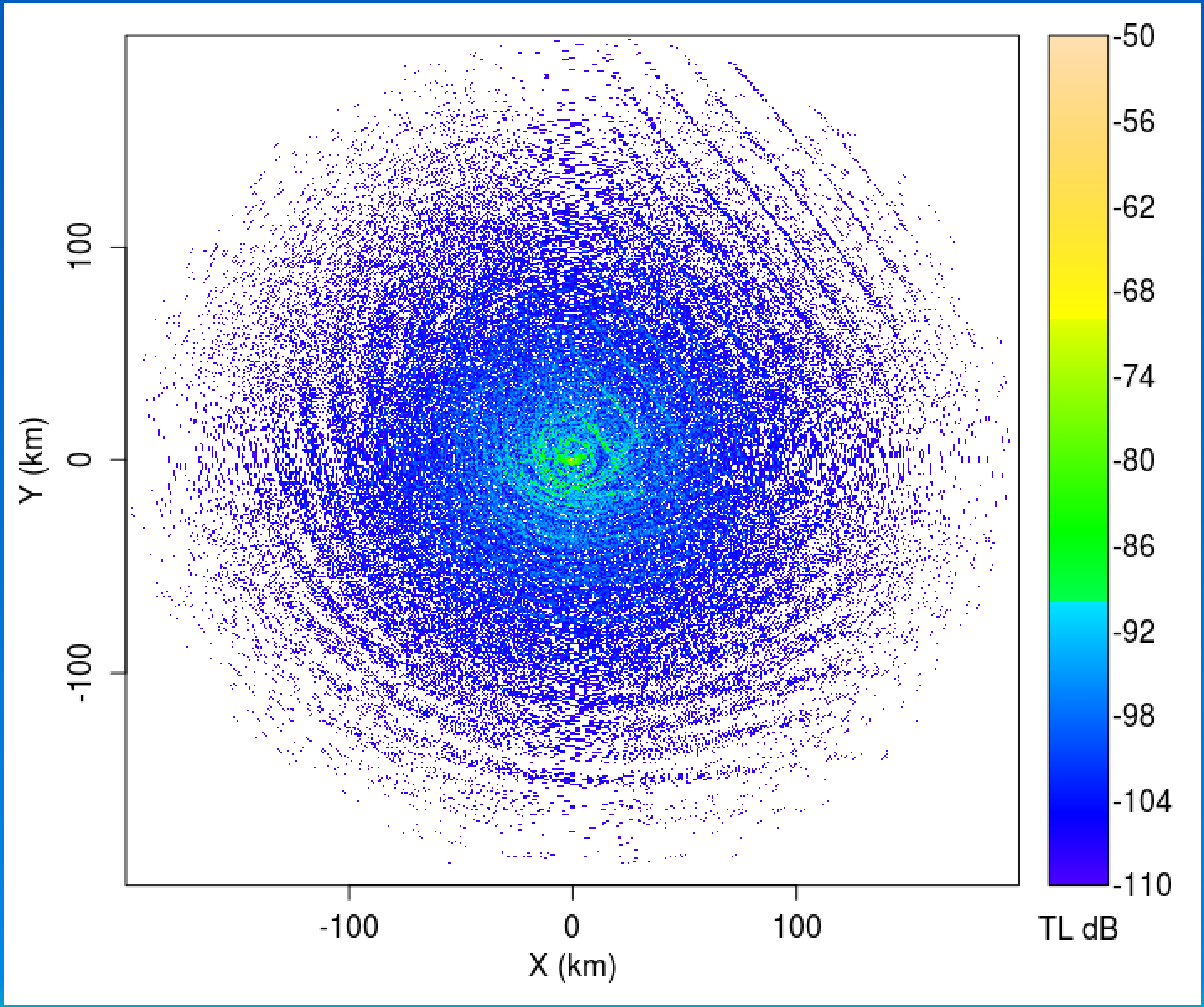

Direction of arrival estimates from phased-array beamforming for the CEPG and Stillwater tornadoes. Red circles and yellow text indicate tornado positions and times. Green lines and text denote direction of arrival and signal analysis times. Times are UTC on May 24, 2011.

Distance	Warning Time (minutes)	
	35 mph	60 mph
10 km	10.2	5.7
20 km	20.4	11.5
30 km	30.6	17.2
40 km	40.8	22.9
100 km	102.0	57.2

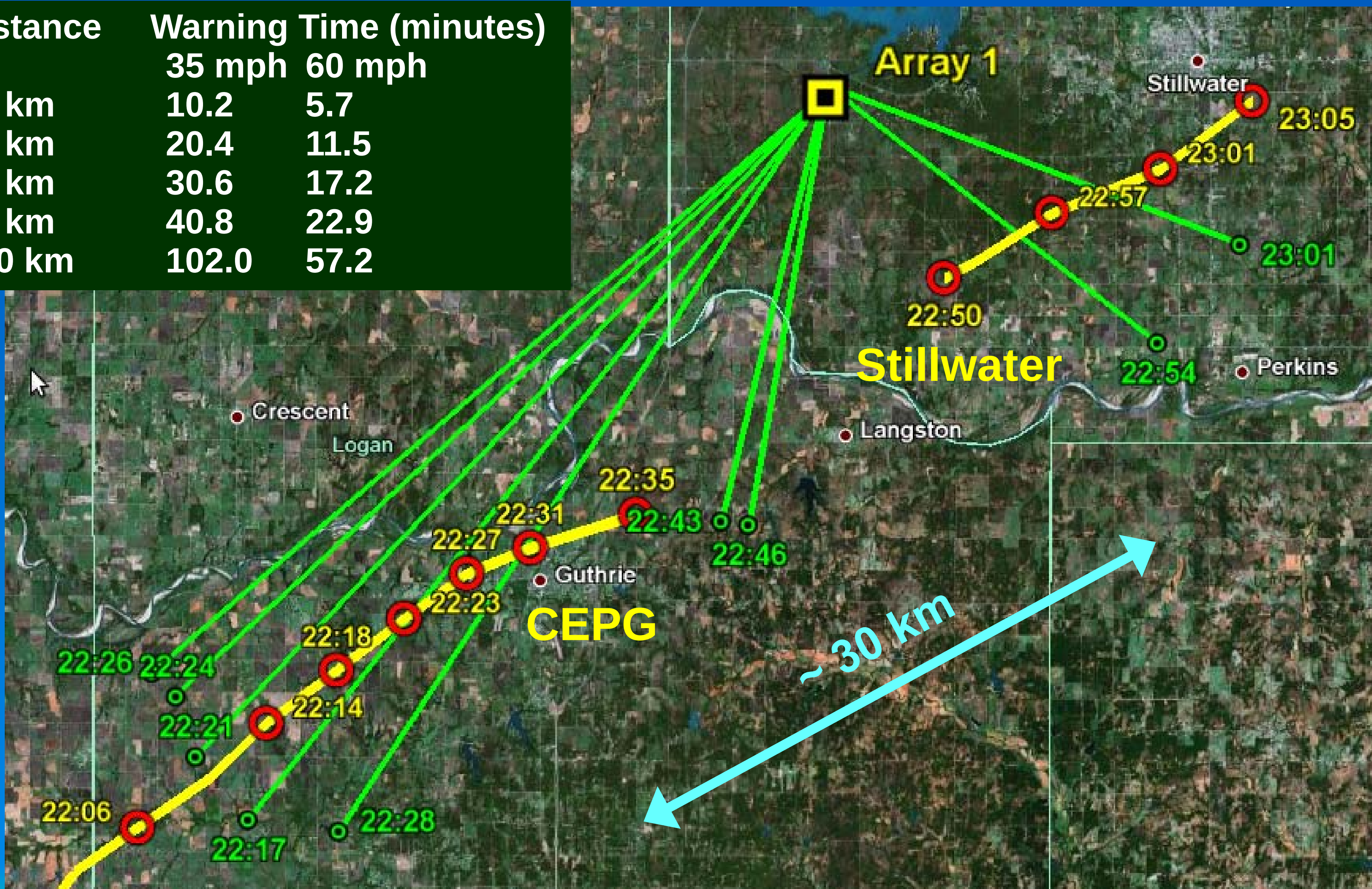

Direction of arrival estimates from phased-array beamforming for the CBN tornado. Red circles and yellow text indicate tornado positions and times. Green lines and text denote direction of arrival and signal analysis times. Times are UTC on May 24, 2011.

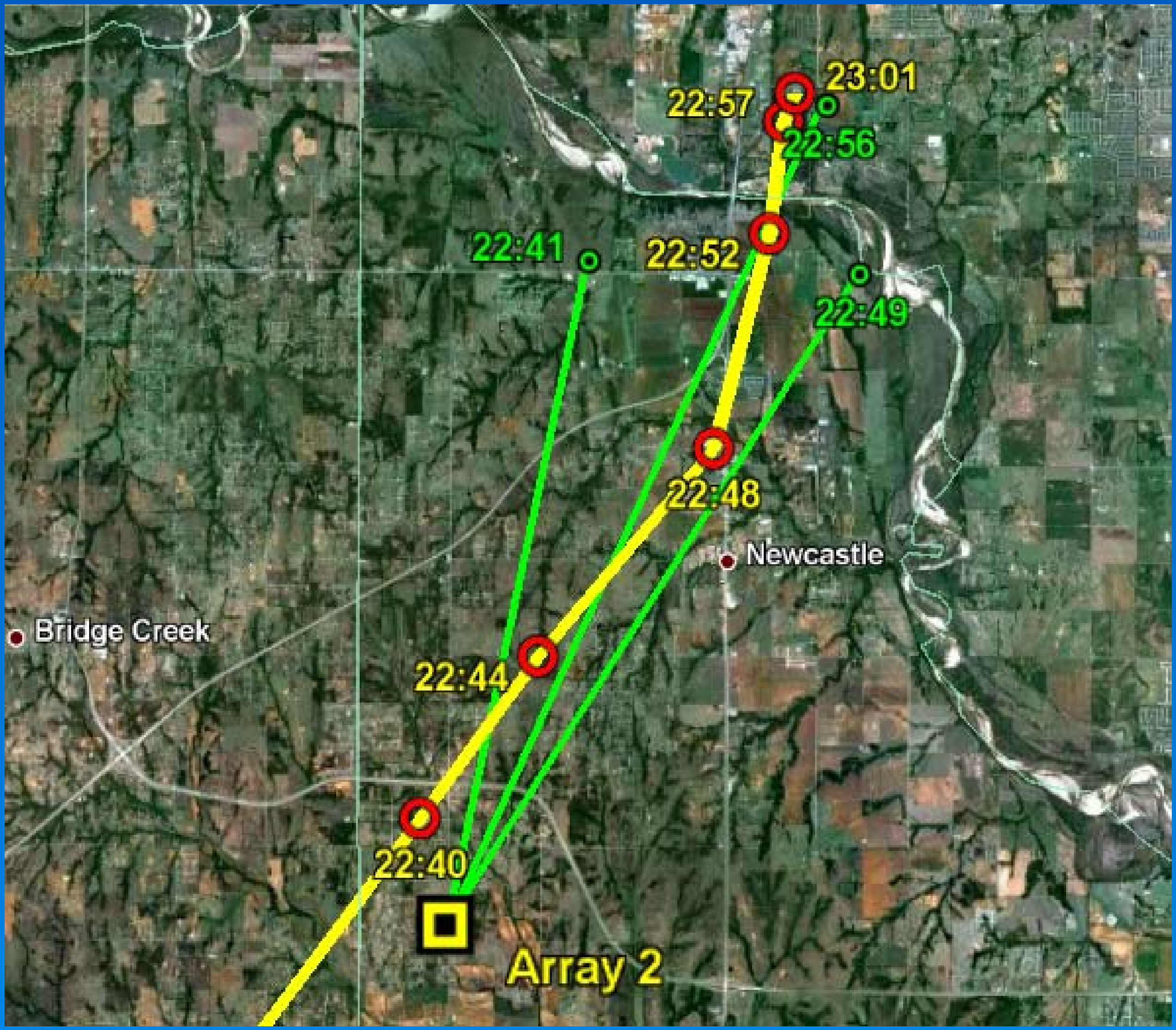

Tornado tracks from the June 20, 2011 Elm Creek (left) and Amherst (right) tornadoes in Nebraska. The approximate location of infrasound sensor arrays is shown by the circles.

June 20, 2011

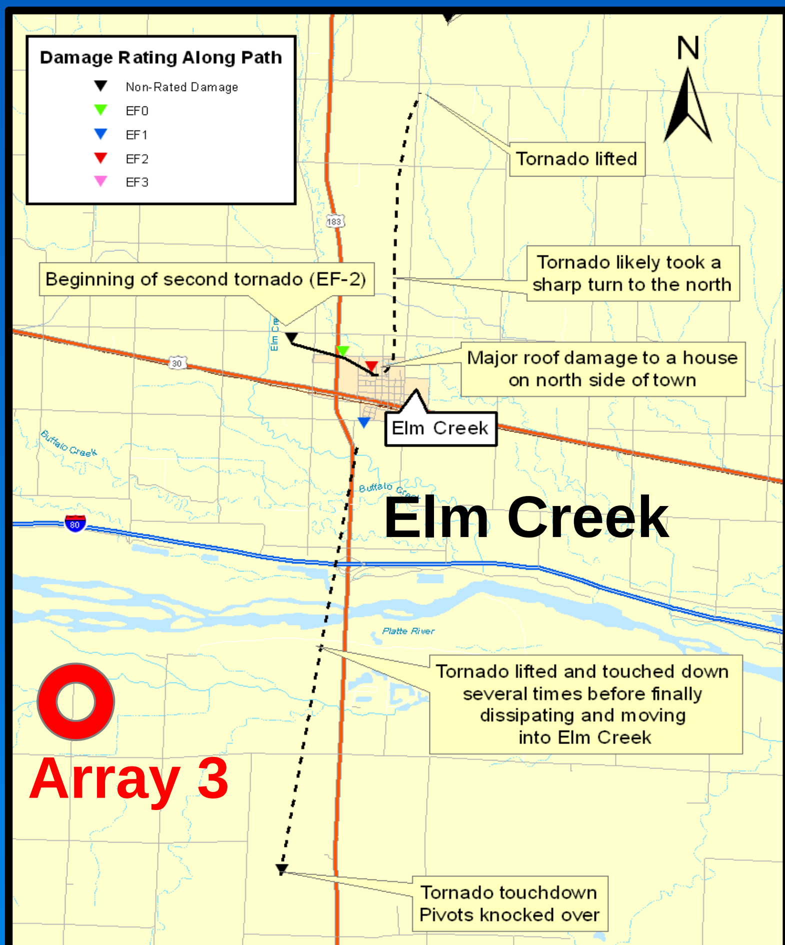

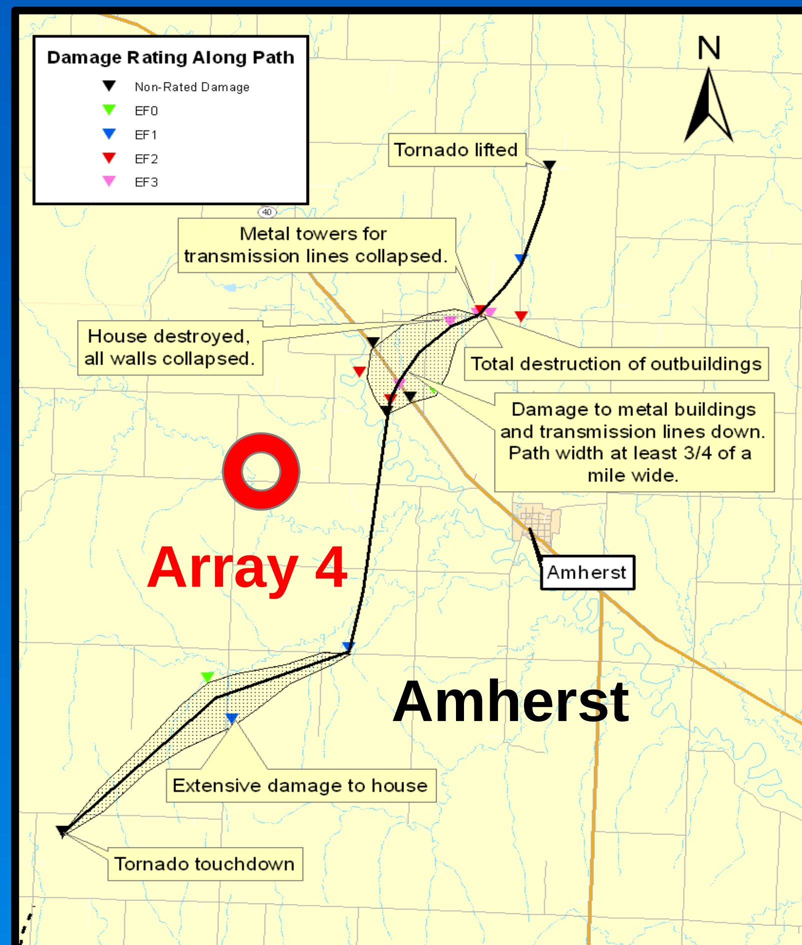

Direction of arrival estimates from phased-array beamforming for the Elm Creek and Amherst tornado. Red circles and yellow text indicate tornado positions and times. Green and magenta lines and text denote direction of arrival and signal analysis times. Times are UTC on June 20, 2011.

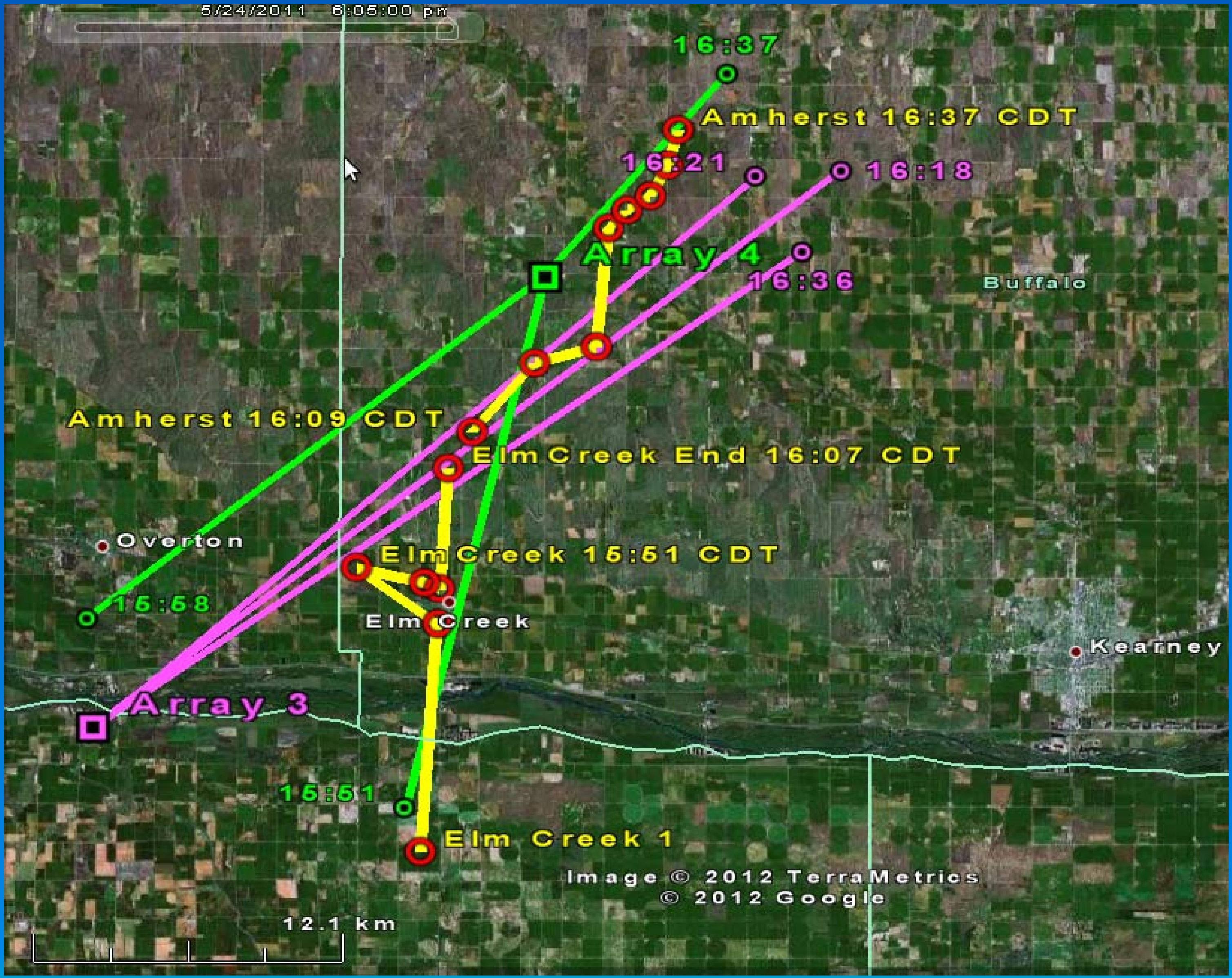

Some Proposed Acoustic Radiation Modes : Bedard

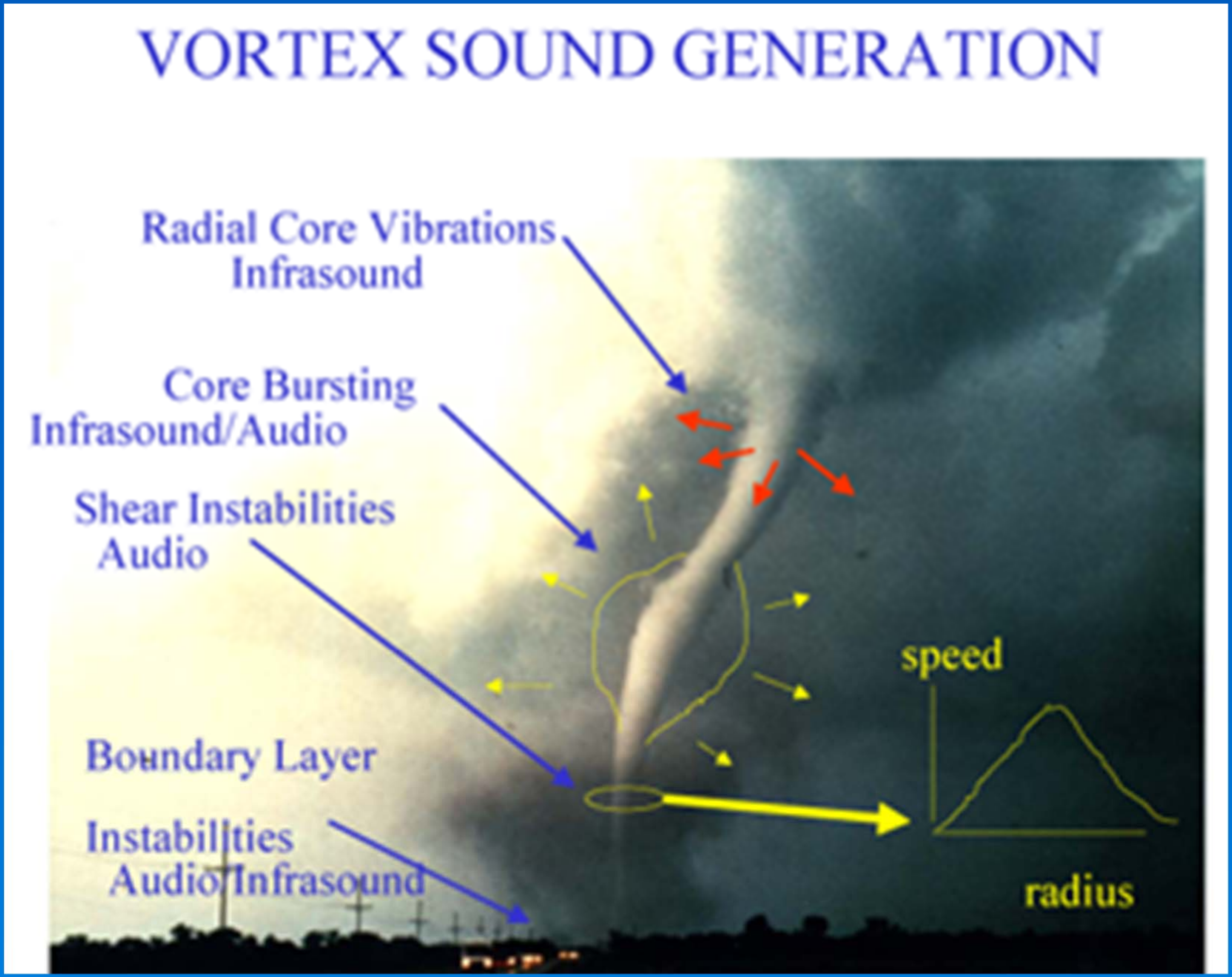

Bedard, A. J., 2005: Low-Frequency Atmospheric Acoustic Energy Associated with Vortices Produced by Thunderstorms. *Mon. Wea. Rev.*, **133**, 241–263.

Schecter, D. A., 2011a: A Brief Critique of a Theory Used to Interpret the Infrasound of Tornadic Thunderstorms, *Monthly Weather Review* 2011

Turbulence

$$E(k) = \alpha\, \varepsilon^{2/3}\, k^{-5/3} \exp[\, -3/2\, \pi\, \beta\, \alpha^{1/2} (k\Lambda)^{-4/3}\,]$$

k = wavenumber
α = scaling coefficient experimentally determined as 1.5
ε = dissipation rate
β = 0.3 constant relating total energy of the spectrum to the square of mean velocity
Λ = length scale of the dominant (energy-containing) eddies

Dissipation rate is estimated from $\varepsilon = u^3 / \Lambda$, where u is the fluid free-stream mean velocity.

Varying u does not change the spectral shape, but controls the energy amplitude.

The shape of the spectrum is dictated by Λ, the value of which can be estimated from the invariance $k\Lambda \approx 1.3$ at the peak of the spectral energy.

Comparison of a 4 sensor averaged PSD from the CEPG storm to a turbulence spectrum computed with a dominant eddy scale of $\Lambda = 2.8$ m ($k\Lambda = 1.3$).
The dashed line plots the turbulence spectrum corrected for frequency dependent acoustic absorption, the dotted line has no absorption correction. Time is UTC on May 24, 2011.

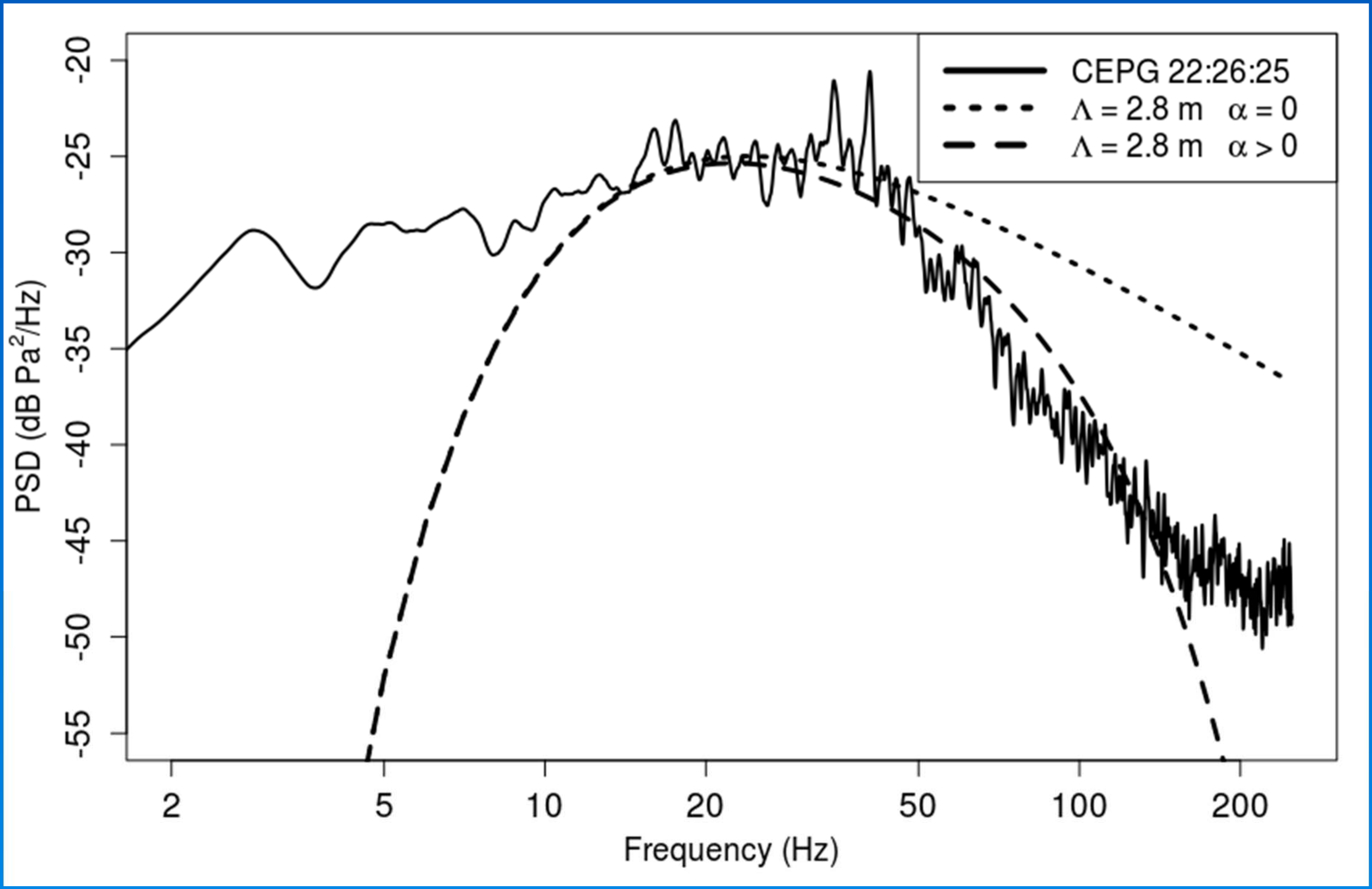

Comparison of a 3 sensor averaged PSD from the CBN storm to a turbulence spectrum computed with a dominant eddy scale of $\Lambda = 0.9$ m.
The dashed line plots the turbulence spectrum corrected for frequency dependent acoustic absorption, the dotted line has no absorption correction. Time is UTC on May 24, 2011.

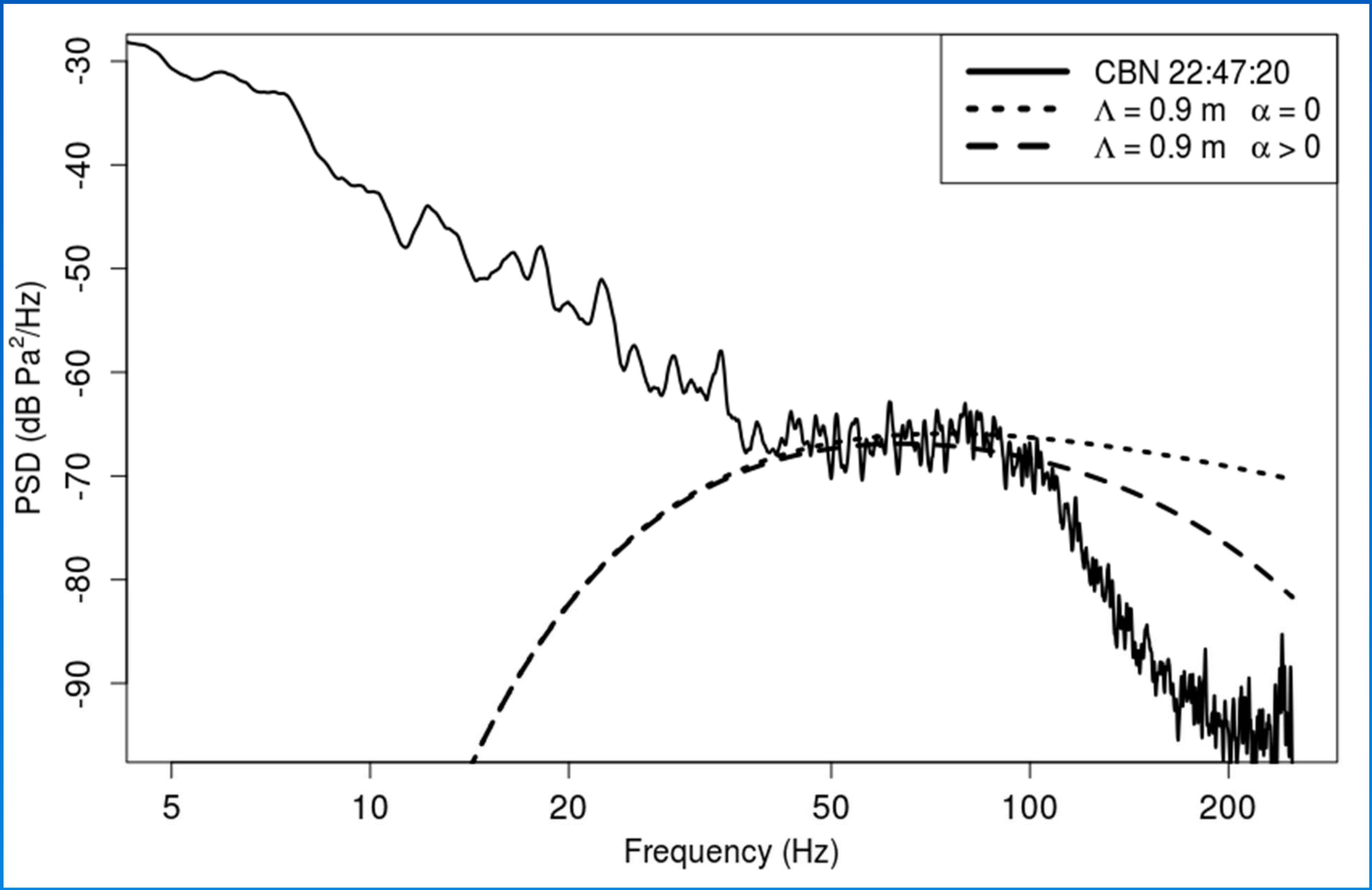

Comparison of a 4 sensor averaged PSD from the Stillwater storm to a turbulence computed with a dominant eddy scale of Λ = 0.75 m.
The dashed line plots the turbulence spectrum corrected for frequency dependent acoustic absorption, the dotted line has no absorption correction. Time is UTC on May 24, 2011.

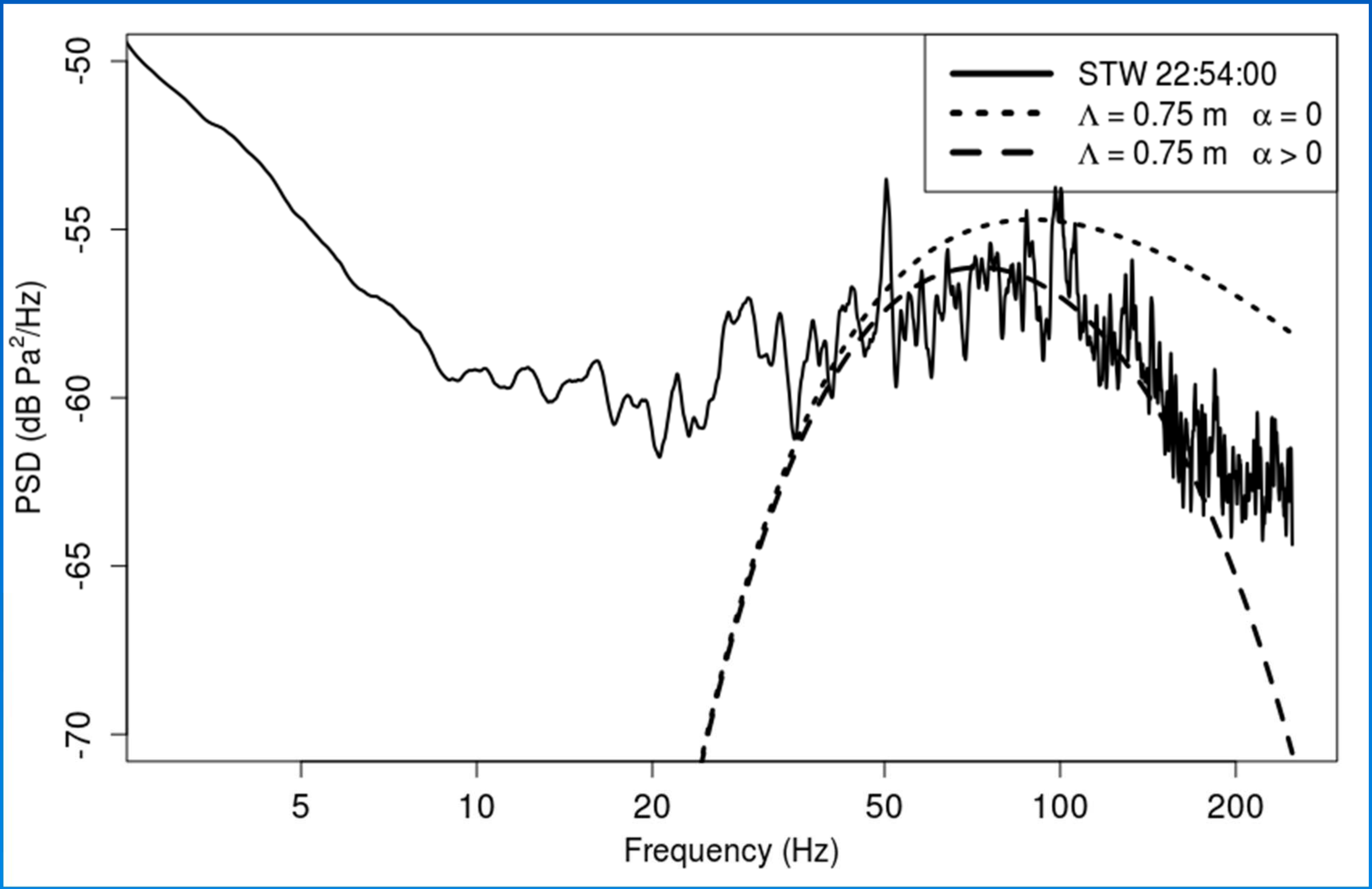

Proposed Application: Regional network of infrasound sensor arrays to compliment NWS Radar.

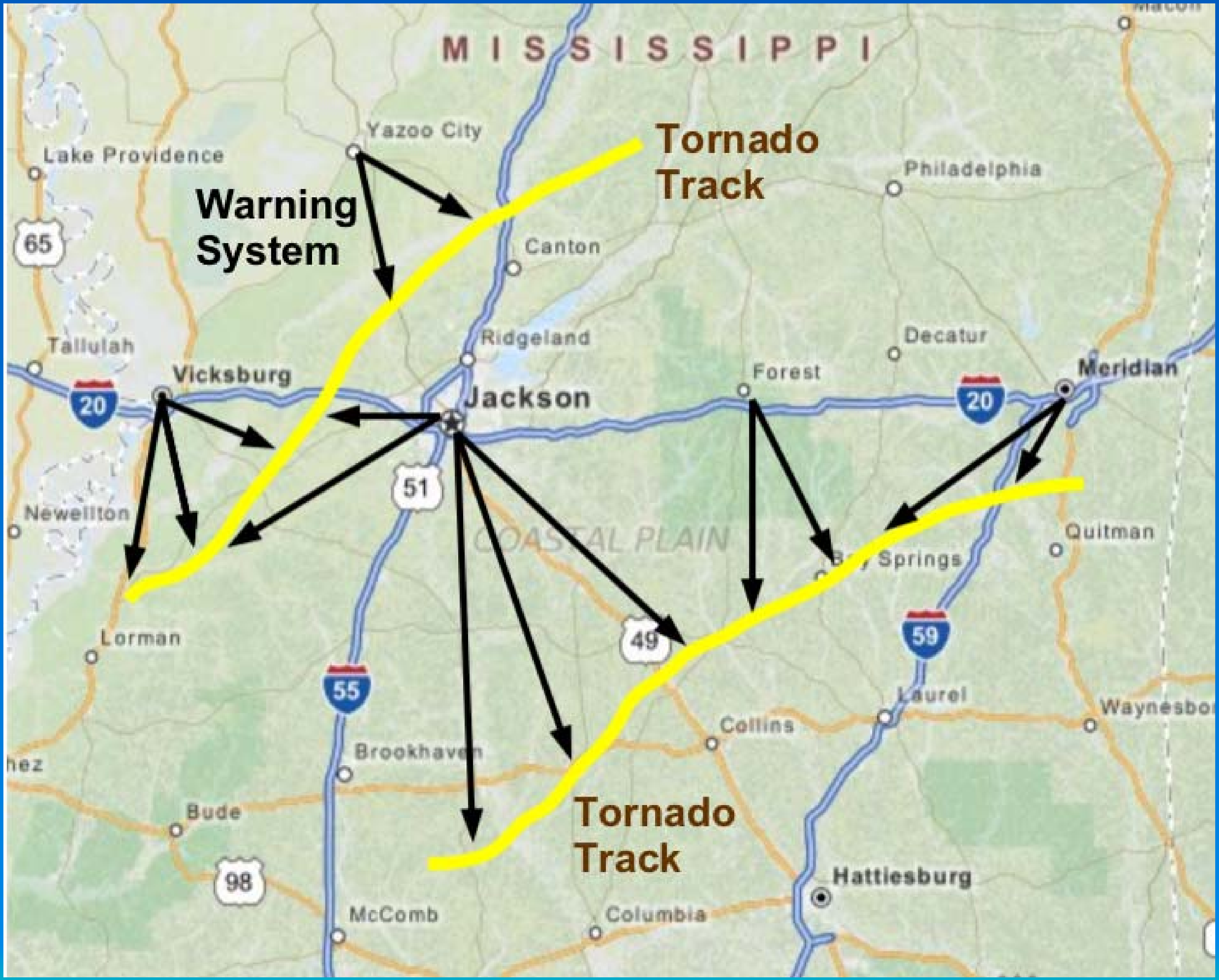

Proposed Application: Monitoring infrasound to compliment NWS Radar.

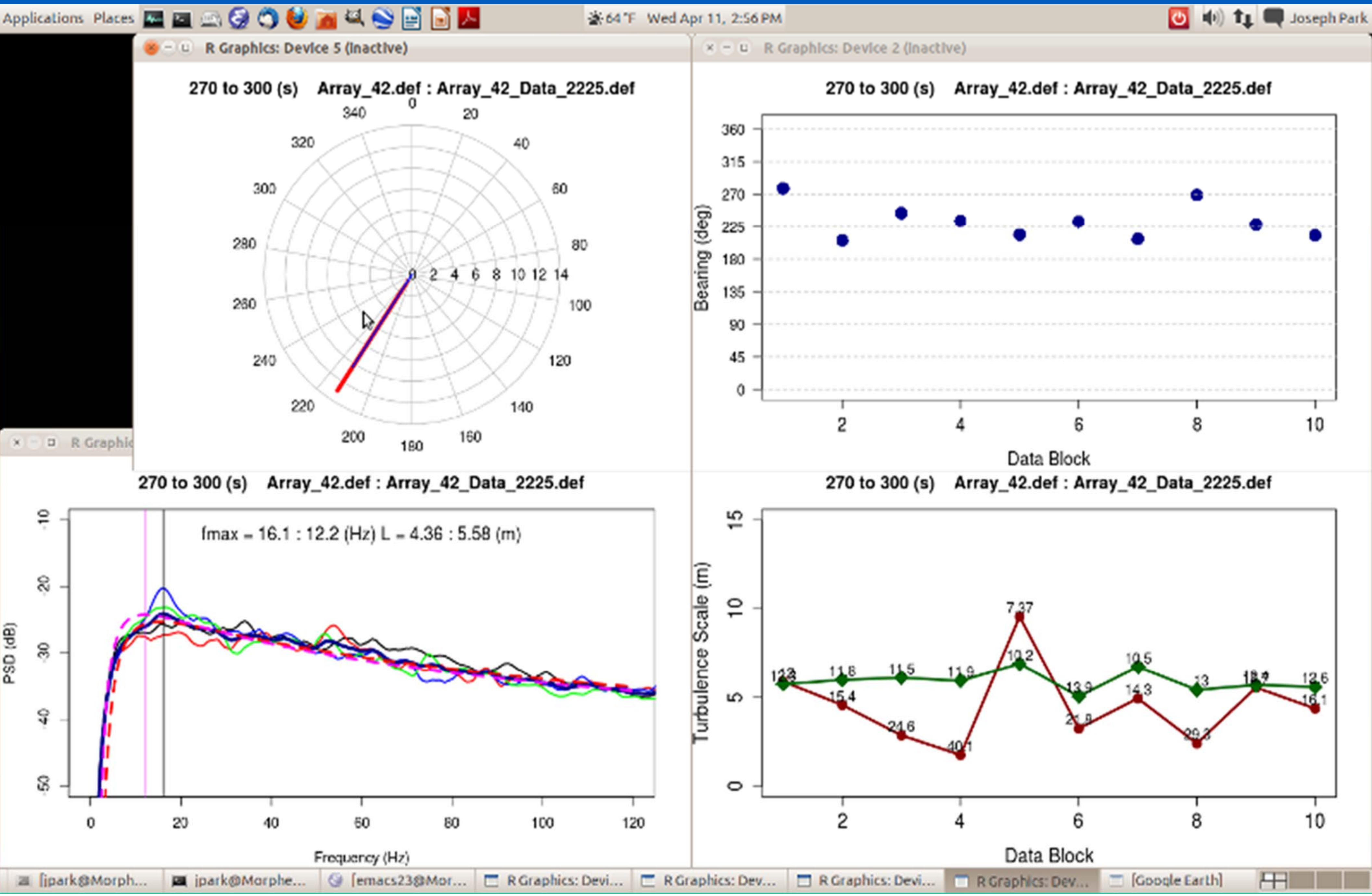

Observations

Tornado acoustic radiation in the infrasonic and sub-audio band is energetic.

Current research attempts to understand the radiation physics.

Tornadoes were detected and tracked using phased-array beamforming up to 113 km from field-deployed infrasound arrays.

Acoustic propagation is roughly 330 m/s, at least 10 times faster than a severe storm (30 m/s = 67 mph), potential warning times are useful.

The acoustic spectral ‘signature’ associated with tornadoes persists between observed tornadoes.

Matching the wavenumber at the peak in the acoustic pressure spectra to the wavenumber of the turbulent energy containing eddies suggests that fluid-dynamical turbulence is a radiation mode.

Connection between the dominant length scale and radiated frequency suggests a means to monitor the dynamics and perhaps intensity.

References

Bedard, A. J., 2005: Low-Frequency Atmospheric Acoustic Energy Associated with Vortices Produced by Thunderstorms. *Mon. Wea. Rev.*, **133**, 241–263. doi: http://dx.doi.org/10.1175/MWR-2851.1

Black, A. W., Walker, S. A., 2011: The Relationship between Tornadic and Nontornadic Convective Wind Fatalities and Warnings. *Wea. Climate Soc.*, **3**, 31–47. doi: http://dx.doi.org/10.1175/2010WCAS1094.1

Bluestein, H. B., 1999: A History of Severe-Storm-Intercept Field Programs. *Wea. Forecasting*, **14**, 558–577. doi: http://dx.doi.org/10.1175/1520-0434(1999)014<0558:AHOSSI>2.0.CO;2

Bradford, M., 1999: Historical Roots of Modern Tornado Forecasts and Warnings. *Wea. Forecasting*, **14**, 484–491. doi: http://dx.doi.org/10.1175/1520-0434(1999)014<0484:HROMTF>2.0.CO;2

Brotzge, J., Erickson, S., Brooks, H., 2011: A 5-yr Climatology of Tornado False Alarms. *Wea. Forecasting*, **26**, 534–544. doi: http://dx.doi.org/10.1175/WAF-D-10-05004.1

Brotzge, J., Erickson, S., 2010: Tornadoes without NWS Warning. *Wea. Forecasting*, **25**, 159–172. doi: http://dx.doi.org/10.1175/2009WAF2222270.1

Coleman, T. A., Pence, K. J., 2009: The Proposed 1883 Holden Tornado Warning System. *Bull. Amer. Meteor. Soc.*, **90**, 1789–1796. doi: http://dx.doi.org/10.1175/2009BAMS2886.1

Georges, T. M., 1973: Infrasound from convective storms: Examining the evidence. *Reviews of Geophysics*, Vol. 11, No. 3, 571-594. doi:10.1029/RG011i003p00571

Georges, T. M., Greene, G. E., 1975: Infrasound from Convective Storms. Part IV. Is It Useful for Storm Warning?. *J. Appl. Meteor.*, **14**, 1303–1316. doi: http://dx.doi.org/10.1175/1520-0450(1975)014<1303:IFCSPI>2.0.CO;2

Kis, A. K., Straka, J. M., 2010: Nocturnal Tornado Climatology. *Wea. Forecasting*, **25**, 545–561. doi: http://dx.doi.org/10.1175/2009WAF2222294.1

National Weather Service, 2009: Storm-based warnings: A presentation for NOAA's NWS managers. URL: http://www.nws.noaa.gov/cfo/program_planning/doc/FY-2009%20NOAA%27s%20NWS%20National%20Performance%20Measures%20-%20Graph%20Update.pdf. Accessed Januray 1st, 2012.

National Weather Service, 2011: Norman Oklahoma, Information for the Tornado Outbreak of May 24, 2011. URL: http://www.srh.noaa.gov/oun/?n=events-20110524, accessed November 30, 2011.

Schecter, D. A., Nicholls, M. E., Persing, J., Bedard, A. J. , Pielke, R. A., 2008: Infrasound Emitted by Tornado-Like Vortices: Basic Theory and a Numerical Comparison to the Acoustic Radiation of a Single-Cell Thunderstorm. *J. Atmos. Sci.*, **65**, 685–713. doi: http://dx.doi.org/10.1175/2007JAS2384.1

Schecter, D. A., Nicholls, M. E., 2010: Generation of Infrasound by Evaporating Hydrometeors in a Cloud Model. *J. Appl. Meteor. Climatol.*, **49**, 664–675. doi: http://dx.doi.org/10.1175/2009JAMC2226.1

Schecter, D. A., 2011: A Method for Diagnosing the Sources of Infrasound in Convective Storm Simulations. *J. Appl. Meteor. Climatol.*, **50**, 2526–2542. doi: http://dx.doi.org/10.1175/JAMC-D-11-010.1

Schecter, D. A., 2011a: A Brief Critique of a Theory Used to Interpret the Infrasound of Tornadic Thunderstorms, *Monthly Weather Review* 2011, doi: http://dx.doi.org/10.1175/MWR-D-11-00194.1

Schecter, D., Nicholls, M., 2011: Simulation and Analysis of Infrasound Generated by Convective Storms and Tornadoes. AGU Fall Meeting 2011, Session A31A, Advances in Atmospheric Infrasound, San Francisco. URL: http://eposters.agu.org/abstracts/simulation-and-analysis-of-infrasound-generated-by-convective-storms-and-tornadoes/. Accessed December 31, 2011.

Talmadge, C. L., Park, J., Waxler, R., Kleinert, D. E., Carter, G. E., Godbold, G., Harris, D. R., Williams, C., 2011: Detection of Infrasonic Energy From Tornado-Producing Storms. AGU Fall Meeting 2011, Session A31A: Advances in Atmospheric Infrasound, San Francisco. URL: http://eposters.agu.org/abstracts/detection-of-infrasonic-energy-from-tornado-producing-storms/. Accessed December 31, 2011.

Tatom, F. B., Knupp, K. R., Vitton, S. J., 1995: Tornado Detection Based on Seismic Signal. *J. Appl. Meteor.*, **34**, 572–582. doi: http://dx.doi.org/10.1175/1520-0450(1995)034<0572:TDBOSS>2.0.CO;2

Tennekes, H. and Lumley, J. L., 1972: *A First Course in Turbulence*, MIT Press, ISBN-13: 978-0-262-20019-6